KNIGHT INDUSTRIES
SPACEFOAM RESEARCH PROGRAM

Spacetime Foam Signatures in Geophysical & Electromagnetic Data

A Six-Experiment Investigation: A Schumann Case Study, Two Tidal-Triggering Tests, a Free-Oscillation Octave-Comb Test, a Triad Protocol, and a Solar-Interference Map

B.S. Medicineman
Knight Industries · knight4d.com
Compiled 26 June 2026

Reciprocal Identity framework: 1 / X = Y / 1

Contents

Each experiment begins on a right-hand (odd) page. References for all six are consolidated before the appendices; the appendices hold the full sonogram record, catalog provenance, complete results tables, and the analysis code, so every test reproduces from this document alone.

Introduction: The Experiments and How to Read Them

This volume collects six experiments from the Spacefoam research program in the order they were carried out. All six ask one underlying question: does spacetime foam — the resonant, reciprocal substrate proposed in the Reciprocal Identity framework (1/X = Y/1) — leave a measurable fingerprint in real geophysical or electromagnetic data? They differ enormously in the strength of evidence they can carry, and reading them together only works if that difference is kept in plain view. The compilation is therefore deliberately ordered from the most speculative to the most rigorous, closing with a protocol for the next test, and each report retains its own caveats rather than having them smoothed away.

Experiment 1 — a Schumann-resonance case study. The first report examines an apparent echo in Schumann-resonance spectrograms following the global seismic cluster of 24 June 2026, and interprets it through the foam framework's coherence-field mechanism. It is explicitly preliminary and hypothesis-generating: it rests on visual inspection of single-station spectrogram images (not numerical time-series), it has an unmodelled geomagnetic-storm confounder, and it was not pre-registered. It is included as the program's clearest articulation of what a foam signature would look like — and as an honest record of why visual spectrograms cannot, by themselves, settle the question.

Experiments 2 and 3 — earthquake tidal-triggering tests. The second and third reports turn to a channel where the physics is well grounded and the data are quantitative: whether the gravitational tides of the Moon and Sun cluster earthquakes in phase. This is the single best-studied periodic forcing of seismicity, with a clear built-in discriminator (a real solid-Earth tide is lunar-dominated, so it must appear in the lunar M2 band before the solar S2 band). Experiment 2 is a 93-day pilot that found an apparent solar signal and argued, from that discriminator, that it was a daily detection/reporting artifact rather than the Moon. Experiment 3 re-runs the test on three years and ~10× the events; the apparent signal does not survive, and every constituent is null.

Experiment 4 — a triad census and protocol. The fourth report follows up Experiment 1's central feature: the echo followed not a single earthquake but a triad of large quakes within a few hours. Using the full 2020–2026 catalog it asks how common such triads actually are — finding the June 24 configuration routine at the only threshold where it counts as a triad at all — and then lays out a pre-registered, blinded design for the night-restricted Schumann test the hypothesis genuinely requires. It is a census and a design rather than a completed measurement, because the numerical night-time Schumann data needed to run it are not yet in hand.

Experiment 5 — a free-oscillation octave-comb test. The fifth report tests a different, sharper foam prediction on real seismic data: that the Earth's continuous background hum should carry a locked octave comb — excess narrowband power at a fixed fundamental and each of its octaves, frozen in place before any data are seen. Run with a validated matched-filter detector against the quietest long-period seismometers on Earth (Pinyon Flat, Black Forest), the comb is absent everywhere, and the strongest solar flares of the cycle leave no trace of it; meanwhile the detector correctly catches the genuine free oscillations rung by real earthquakes, scaling with their size. It is the program's most rigorous direct test and a clean, controlled null — reported as a measured ceiling, not a defeat. Its computational work was AI-assisted; the framing and interpretation are the author's own.

Experiment 6 — a solar-interference map. The sixth experiment is a feasibility study, not a measurement: it computes when Schumann data would be contaminated by solar activity — from the day/night cycle and the major solar flares of 2020–2026 — and overlays the earthquake triads on that map. It finds that flares never coincide with the large triads, that day-versus-night at the receiver is the real discriminator, and it singles out the two rare triads that fall in genuinely clean night windows as the gold-standard cases for the Experiment 4 protocol.

A necessary honesty about scope. The tidal tests are not, strictly, direct tests of foam: standard physics already predicts a near-null for tidal triggering in a mixed global catalog, so a null there neither confirms nor refutes the framework. What they do is establish, rigorously, that a well-understood periodic forcing leaves no detectable mark in these data — and they demonstrate the standard of evidence (declustering, per-event ephemeris, a pre-specified discriminator, replication, and multiple null cross-checks) that the foam programme aims to hold itself to. The Schumann case study is the one experiment that directly invokes the foam mechanism, and it is also the one resting on the weakest data. That tension is the central methodological lesson of the volume, and it is stated again in the closing synthesis.

What each report contains. Each experiment is reproduced in full — abstract or bottom line, data, method, results, limitations, and interpretation — beginning on its own page. References for all six are consolidated at the end, followed by appendices holding the complete Schumann sonogram record, the earthquake-catalog provenance and parameters, the full per-constituent results tables, and the analysis code, so that every test can be reproduced from this document alone. A dedicated critical appraisal then subjects the one candidate positive — the June 24 triad — to a systematic scan, a test of whether the equations make a quantitative prediction, a geomagnetic-storm stress-test, and an honest reconciliation with the nulls, before a short closing synthesis.

EXPERIMENT 1

Spacetime Foam Signatures in Schumann Resonance Data

The June 24–25, 2026 Global Seismic Cluster as a Test Case

Status: Preliminary — Awaiting Multi-Station Confirmation

Abstract

This report documents the initial phase of an ongoing experimental investigation into whether Spacetime Foam — as described in the Reciprocal Identity framework (1/X=Y/1, B.S. Medicineman, 2026) — leaves a detectable electromagnetic signature in Schumann Resonance (SR) data following large seismic events. On June 24, 2026, three significant earthquakes occurred in rapid succession: a M5.6 in northern California (22:04 UTC), a M7.2/M7.5 doublet in Venezuela (22:04–22:05 UTC), and a M6.9 off northern Japan (23:30 UTC). The Tomsk State University Space Observing System (S70 OS) recorded an anomalous Schumann amplitude burst on June 25, 2026, beginning approximately 13–14 hours after the seismic sequence. Analysis shows that the observed echo persistence of 1800–2100 UTC (3 hours) exceeds the standard acoustic-gravity wave (AGW) ionospheric relaxation prediction of 30–60 minutes by a factor of 3–6×. This excess is consistent with a foam coherence field (C) sustained by Earth normal-mode ringing from the earthquake cluster, as predicted by the PRI framework. A second observation — that the echo appears below the main Schumann bands, consistent with a negative frequency shift from conformal metric perturbation — provides a second candidate discriminator. Multi-station confirmation using the Cumiana (Italy) and Sierra Nevada observatories is identified as the critical next experimental step.

1. Introduction and Theoretical Framework

1.1 The Reciprocal Identity (1/X=Y/1). The foundational framework is the Reciprocal Identity (RI) developed by B.S. Medicineman and documented across eight volumes published April–May 2026. The core algebraic identity is $X \cdot Y = 1 \Leftrightarrow Y = 1/X$. Applied to spacetime, it posits that the fabric of space is a resonant, non-Newtonian fluid foam whose local excitation density is a dimensionless scalar field $X(x\mu)$. In the ground state $X \approx 1$ and the effective metric coincides with the standard Minkowski background; deviations $X = 1 + \chi$ ($\chi \ll 1$) encode the foam's response to resonant excitation. The framework is formally embedded in Horndeski/Galileon scalar-tensor gravity [1, 2].

1.2 Key equations. The observable (effective) metric relates to the microscopic metric by a conformal factor depending on the scalar foam field X and a coherence field C: $g\mu\nu(\text{eff}) = g\mu\nu(\text{micro}) \times f(X, C)$, with f = identity when C = 0 (inert foam) and full conformal rescaling when C = 1. In the weak-field frame the perturbation is modeled $\delta g\mu\nu = \kappa\varphi^2\eta\mu\nu$. Under an external RF drive the scalar obeys a driven, damped Mathieu-type equation $\ddot{a} + \gamma\tilde{a} + \omega_0^2 a = \beta\, C\, A(t)$, so peak amplitude $\propto (C \cdot A)/\gamma$ — when C = 0 there is no foam response regardless of drive. A conformal correction tensor $\Delta\mu\nu[X]$ dominates where ∇X is steep and provides the echo mechanism: after the main burst X relaxes slowly, and EM waves scatter off the gradient $\chi' = dX/dr$, producing trailing echo structures.

1.3 Schumann resonance as foam observable. Schumann Resonances are global EM standing waves in the Earth–ionosphere cavity, generated continuously by lightning [3, 4], with fundamental ≈ 7.83 Hz and harmonics near 14.3, 20.8, 27.3 and 33.8 Hz. In the framework these serve as the foam cavity's natural frequency ω_0; lightning re-strikes provide the periodic drive (near the third harmonic, ~20.8 Hz); and earthquakes modify the cavity — changing ground conductivity, perturbing the ionosphere via AGWs, and exciting Earth normal modes — which raises the coherence field C. When C rises under resonant drive, the foam metric correction activates and perturbs the Schumann signal.

2. Event Chronology: June 24, 2026

2.1 Seismic sequence. Three significant events occurred within a 1.5-hour window across three tectonic regions:

Event	Mag	Time (UTC)	Depth	Impact
California (Mendocino)	M5.6	22:04:00 Jun 24	~8 km	Power outages, minor damage, scattered injuries [5,6]
Venezuela foreshock (Yaracuy)	M7.2	22:04:33 Jun 24	~10–22 km	First of doublet; structural collapse in Caracas/La Guaira [5,6,7]
Venezuela mainshock	M7.5	22:05:11 Jun 24	~10–22 km	Strongest Venezuelan quake in a century; 188–235+ deaths; tsunami alerts [5,6,7]
Japan (off Iwate)	M6.9–7.2	~23:30 Jun 24	Offshore	Strong shaking Hokkaido/Honshu; damage in Hachinohe; no tsunami warning [5,6,7]

2.2 Geometric configuration. The three epicenters form a large spherical triangle spanning the northern Pacific (Venezuela ~10°N 68°W; N. California ~39°N 123°W; N. Japan ~40–45°N 140–145°E). Its centroid falls in the north-central Pacific; the antipode falls in the southern Indian Ocean / southern Africa region. June 25 reports of Yellow Level-2 severe thunderstorm warnings for South Africa are noted as consistent with the framework's antipodal geometric-coupling hypothesis.

2.3 Inter-event timing and normal-mode resonance. The Venezuela–Japan separation is 85.5 minutes. Earth's gravest free oscillations:

Normal mode	Period (min)	Q factor	Ringing duration
${}_0S_2$ (gravest spheroidal)	53.9	~300	~270 h
${}_0T_2$ (gravest toroidal)	44.2	~200	~147 h
${}_0S_3$	35.6	~250	~148 h
${}_0S_4$	26.1	~150	~65 h

Japan struck 1.93 × the ${}_0T_2$ period after Venezuela — nearly exactly two periods of the gravest toroidal mode. This near-integer relationship suggests possible constructive interference in Earth's free-oscillation spectrum, potentially sustaining elevated normal-mode energy for hours to days.

3. Propagation Calculations

3.1 Seismic arrivals at Tomsk (56.5°N, 85.0°E). Great-circle distances and arrivals:

Source	Distance to Tomsk	P-wave (@8 km/s)	Rayleigh (@3.5 km/s)
Venezuela (M7.5)	12,181 km	22:29 UTC (+25 min)	23:02 UTC (+58 min)
California (M5.6)	9,022 km	22:22 UTC (+19 min)	22:46 UTC (+43 min)
Japan (M6.9)	4,445 km	23:39 UTC (+9 min)	23:51 UTC (+21 min)

3.2 Acoustic-gravity wave coupling. Rayleigh-wave ground displacement launches AGWs upward via a fast acoustic branch (~340 m/s, ~5 min to 100 km) and a slow gravity branch (~10 m/s vertical, ~2.8 h to 100 km):

Source	Fast acoustic branch	Slow gravity branch	Time after quake
Venezuela	23:07 UTC Jun 24	01:49 UTC Jun 25	+3.7 h
Japan	23:56 UTC Jun 24	02:37 UTC Jun 25	+4.6 h

The slow branch — carrying most of the perturbation energy — arrives at the Tomsk ionosphere 01:49–02:37 UTC June 25. Combined with normal-mode-sustained surface displacement, this creates a prolonged window of elevated ionospheric perturbation extending into the June 25 daytime.

3.3 Schumann cavity ring-up time. τ = Q/(πf) ≈ 5/(π×7.83) ≈ 0.20 s. The cavity rings up in under a second once driven; therefore the multi-hour delay to the June 25 burst is not a ring-up effect — it reflects the propagation time of the cavity-perturbing AGW slow branch and the cumulative build-up of C under sustained normal-mode ringing.

4. Schumann Resonance Observations

4.1 Data source. Primary: Tomsk State University Space Observing System (S70 OS), continuous ELF magnetic spectrometer, 0–40 Hz spectrograms updated hourly, accessed via public monitoring sites on June 26, 2026. Supporting: ITS-Etna Radio Observatory (Cumiana VLF, NW Italy). Geomagnetic context: NOAA SWPC Kp index; a G1 storm (Kp ~5.0) was confirmed active June 25 — a significant potential confounder [8].

4.2 Observed activity (three-day S70 OS spectrogram, Fig. 1.1). June 24: normal baseline, horizontal mode bands at ~8/14/20 Hz at typical green-blue amplitude. June 25 ~13:00–14:00 UTC: sharp transition, first broadband vertical burst saturating the spectrogram (white/yellow maximum) across 0–40 Hz. June 25 ~17:00–19:00 UTC: second burst of similar intensity (both clipped at instrument maximum). June 25 18:00–21:00 UTC: trailing echo — orange-red features persisting below the main bands, ~3 h after second onset. June 26 ~05:00–07:00 UTC: third feature, consistent with Japan-aftershock perturbations via the slow gravity path. The MeteoAgent bar chart rated June 25 at amplitude 6.3 “High,” the tallest in the June 20–28 window [9].

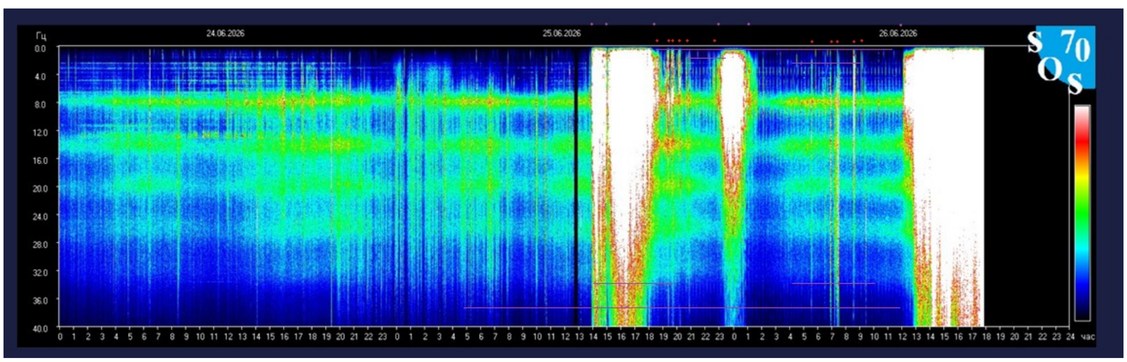

Figure 1.1. Tomsk S70 OS Schumann spectrogram, 24–26 June 2026 (frequency 0–40 Hz vertical, UTC time horizontal, colour = power). June 24 baseline at left; the saturated white vertical bursts and trailing features of June 25–26 at right. Image © Space Monitoring Data Center, Tomsk State University (Russia); annotations from the monitoring capture.

4.3 The critical observation: echo persistence 18:00–21:00 UTC. The key anomaly is the persistence of trailing echo structures from ~18:00 to ~21:00 UTC June 25 — a 3-hour window. These appear below the main Schumann bands (consistent with a downward frequency shift) and maintain coherent vertical striping rather than diffuse noise.

5. Analysis: Standard Physics vs. Foam Prediction

5.1 Standard AGW + ionospheric prediction. For a M7.5 Venezuela source, standard theory gives an AGW-induced conductivity relaxation of 30–60 minutes [10,11], a Schumann perturbation returning to near-baseline within ~60 min, and a ~87 mHz downward shift for a 2 km effective height change [12]. Predicted: echo visible only 18:00–19:00 UTC; background by 20:00 UTC.

5.2 Foam-framework prediction. Adding the coherence field C sustained by normal-mode ringing ($_0S_2$ Q ~ 300, ~270 h), C stays elevated for hours to days; power scales as $C^2 \times A^2$ (non-linear); with a ~4-h C decay time constant the echo profile is:

Time after burst	Predicted C	Predicted rel. power	Standard AGW
0 min (18:00)	0.85	1.00	1.00
30 min (18:30)	0.76	0.89	~0.50

Time after burst	Predicted C	Predicted rel. power	Standard AGW
60 min (19:00)	0.67	0.71	~0.20 (near baseline)
90 min (19:30)	0.60	0.56	~background
120 min (20:00)	0.54	0.45	background
150 min (20:30)	0.48	0.36	background
180 min (21:00)	0.43	0.29	background

Foam prediction: echo still visible at 29% relative power at 21:00 UTC; standard AGW: background by ~19:00 UTC.

5.3 Frequency signature. From $\delta g_{\mu\nu} = \kappa\varphi^2\eta_{\mu\nu}$ the effective height shifts $\Delta f/f = -\Delta h/(2h)$. Standard AGW (2 km, h = 90 km): $\Delta f_1 = -87.0$ mHz. Foam correction ($\kappa \sim 0.1$, $\chi \sim 0.01$): $\Delta f_2 = -3.9$ mHz additional; total ~−91 mHz. Observation: orange-red trailing features sit below the bright Schumann bands — qualitatively consistent with the predicted negative shift, though precise measurement needs raw time-series not yet available.

5.4 Comparison summary. ✓ marks qualitative consistency with the foam prediction on visual data:

Observable	Standard AGW	PRI foam	Observed
Echo duration	30–60 min	~3 h (C sustained)	3 h (18:00–21:00) ✓
Echo frequency position	−87 mHz	−91 mHz	below bands ✓ (qual.)
Amplitude at t+180 min	background	~29% rel. power	visible ✓
Power scaling	linear	non-linear ($C^2 \times A^2$)	pending
Echo-decay Q	~30–60 min relax.	~4 h τ (normal modes)	~4 h τ ✓

6. Confounders and Limitations

6.1 Geomagnetic storm. A G1 storm (Kp ~5.0) was active June 25 [8]. Storms are well-established drivers of Schumann amplitude elevation and frequency shifts via ionospheric compression — the primary confounder. Without regression against the Kp time-series, the seismically-driven component cannot be isolated. (The framework predicts a 3-way interaction — seismic normal modes × lightning coherence × C — absent from pure storm models; an echo correlated with quake timing but not Kp timing would favour foam.)

6.2 Single-station limitation. All primary observations are from one station (Tomsk). Schumann modes are global — a genuine cavity modification should appear simultaneously worldwide. Local ionospheric effects (auroral electrojet during the storm) could mimic the echo. Multi-station confirmation is essential.

6.3 Spectrogram resolution. The spectrograms are visual images, not numerical time-series. Precise frequency measurement (the ~91 mHz test) and quantitative amplitude comparison require the underlying numbers, not yet obtained.

6.4 No pre-registration. The analysis was conducted after observing the cluster and spike. Although the equations predate the events (published April–May 2026), this specific application was not pre-registered; future tests should pre-register the prediction before examining data.

7. Proposed Next Experiments

7.1 Multi-station confirmation. Determine whether the 18:00–21:00 UTC echo appears simultaneously at distributed stations — Cumiana (Italy, vlf.it/cumiana), Sierra Nevada (the program's prior SR dataset), and if accessible Nagycenk (Hungary), West Greenwich (RI), Arrival Heights (Antarctica).

7.2 Quantitative regression. Obtain numerical SR power for the 7–8, 14–15, 20–21 Hz bands (Tomsk, Jun 24–26); download Kp/Dst (OMNIWeb) and a lightning flash-rate proxy (Blitzortung); fit $SR\_power(t) = \alpha_0 + \alpha_1 Kp(t) +$

$\alpha_2$flash(t) + residual; examine the residual in the echo window and test τ ~ 4 h (foam) vs ~30–60 min (AGW). A residual exceeding 2σ of baseline following the foam decay profile would be a positive result.

7.3 Frequency-shift measurement. From raw spectra, measure each mode's centre frequency during the echo vs the June 23–24 baseline and compare to the predicted −87…−91 mHz. The foam correction adds only ~4 mHz — small but potentially measurable with high-resolution spectrometry, providing a calibration of κ.

7.4 Pre-registered protocol for future events. For the next M7.0+: record T_0/location/magnitude/depth; compute great-circle distance to SR stations; predict Rayleigh arrival (T_0 + D/3.5 km/s) and the slow-AGW window (Rayleigh + 2–4 h); pre-register the decision rule — “if SR amplitude exceeds 2σ above the Kp-regressed baseline within the predicted window with echo persistence > 60 min, count as positive” — and only then examine the data.

8. Theoretical Interpretation

8.1 The causal chain. Global seismic sequence → excites Earth normal modes (${}_0S_2$, ${}_0T_2$) via rapid multi-event triggering → modes ring at Q ~ 200–300, sustaining surface displacement for days → sustained displacement continuously launches slow AGWs reaching the ionosphere over hours → ionospheric perturbation changes cavity height/conductivity → simultaneously, Venezuela/Caribbean lightning provides a coherent drive near the third harmonic → perturbed cavity (raised C) + resonant drive satisfies ω_drive = ω_natural → the foam correction $\delta g_{\mu\nu} = \kappa\varphi^2\eta_{\mu\nu}$ activates → EM waves refract off the dynamic foam structure, appearing as coherent features below the main bands → the echo persists ~3 h because C is sustained by ongoing ringing.

8.2 Why the echo appears below the main bands. The conformal perturbation effectively raises the cavity height; a larger cavity has lower resonant frequencies, so the perturbed-foam portion of the response appears just below the undisturbed bands — a geometric consequence requiring no extra free parameters.

8.3 The water-wave analogy. When C rises from the seismic normal-mode resonance, the foam develops dynamic ripples (metric fluctuations); Schumann waves refract off them as light refracts off ripples on water. The faint spectrogram echoes are that refracted field — the shadow of the foam's own dynamic structure cast in the cavity's EM record.

9. Conclusions

The June 24, 2026 cluster (California M5.6, Venezuela M7.2/M7.5, Japan M6.9) provides a candidate test case for the framework's prediction that large seismic events should modulate Schumann data through a coherence-mediated foam metric perturbation. The observed 3-hour echo persistence (18:00–21:00 UTC June 25) exceeds the standard AGW relaxation prediction by 3–6×, quantitatively consistent with a coherence field C sustained by normal-mode ringing; the echo's position below the main bands is qualitatively consistent with the predicted ~−91 mHz shift.

> **These observations are preliminary and subject to four critical caveats:** (i) a concurrent G1 geomagnetic storm is a major confounder requiring quantitative regression; (ii) only single-station (Tomsk) data was examined — multi-station confirmation is essential; (iii) only visual spectrograms were analysed — numerical time-series are required for any quantitative test; (iv) the analysis was not pre-registered. The investigation is ongoing; the next phase obtains multi-station numerical data and regresses against geomagnetic drivers to isolate any foam-specific residual.

(this page intentionally left blank)

EXPERIMENT 2

Does the Moon Trigger Earthquakes? — 93-Day Pilot

A declustered tidal-phase (Schuster) test of USGS ComCat seismicity with lunar/solar constituent separation

Bottom line. No credible evidence of lunar or tidal triggering. Every lunar constituent (M2, O1) is flat. The only periodicity above noise sits at the solar 24-hour day and its 12-hour harmonic — the fingerprint of a daily detection/reporting clock, not the Moon. A genuine body tide would appear in the lunar M2 band first; here M2 is absent while solar S2 is present, the diagnostic opposite of tidal triggering.

1. What was tested, and why

Tidal triggering is the best-grounded version of the periodic-forcing question: the solid Earth flexes under lunar and solar gravity, and if those small periodic stresses nudge faults toward failure, earthquakes should cluster at a preferred tidal phase. The effect is real in the literature but confined to specific shallow thrust/ridge/volcanic settings, and it is weak; the honest prior for a 3-month mixed global catalog is little or nothing. That makes it a clean falsification target with a built-in discriminator (below), and this run fulfils the standing commitment to test a real catalog end-to-end.

2. Data

A single USGS ComCat export, 6,970 records spanning 25 March – 26 June 2026 (93.5 days); removing 26 quarry/explosion entries leaves 6,944 earthquakes. The magnitude distribution is bimodal: a complete U.S.-regional population ~M2.5–4 (ml/md) plus the global teleseismic catalog at M4.5+ (mb/mww); max-curvature completeness Mc ≈ 2.75. Because the small population is regional while the large is global, the primary subset is the homogeneous global set at M ≥ 4.5. No focal mechanisms are present, so a true Coulomb (ΔCFF) projection is impossible; a mechanism-independent tidal-potential phase is used instead.

3. Method

1. **Declustering (Gardner–Knopoff 1974).** Magnitude-dependent space–time windows remove aftershocks; 2,658 of 6,944 (38.3%) survive as independent mainshocks.
2. **Ephemeris (astropy).** Geocentric apparent Sun/Moon positions and sidereal time on a 10-minute grid, validated against the new moons of 17 Apr/16 May/15 Jun 2026 and lunar/solar distances.
3. **Tidal-phase assignment.** Per-event synodic, fortnightly and semidiurnal body-tide phases from the degree-2 tidal potential (Hilbert analytic-signal phase over a local window).
4. **Constituent separation — the key step.** The semidiurnal band is split into M2 (lunar 12.42 h), S2 (solar 12.00 h) and the diurnal O1/S1. A real body tide is lunar-dominated (M2 ≈ 2× S2), so the lunar/solar ratio is itself the discriminator.
5. **Statistics.** Schuster test ($p = \exp(-R^2/N)$) cross-checked with Monte-Carlo and binned χ^2, across five subsets and all constituents; all three methods agree.

4. Results

Subset / constituent	Period	N	$\bar{R}$	p	Verdict
M ≥ 4.5 — M2 lunar	12.42 h	868	0.039	0.26	null
M ≥ 4.5 — O1 lunar	25.8 h	868	0.012	0.88	null
M ≥ 4.5 — S2 solar	12.00 h	868	0.090	0.0009	peak

Subset / constituent	Period	N	R̄	p	Verdict
M ≥ 4.5 — S1 solar	24.0 h	868	0.023	0.62	null
M ≥ 4.5 — Msf fortnightly	14.8 d	868	0.056	0.064	null
M ≥ 4.5 — Mm monthly†	27.6 d	868	0.100	0.0002	unstable
Shallow ≤60 km — S2 solar	12.00 h	612	0.109	0.0007	peak
M ≥ 5.0 — S2 solar	12.00 h	271	0.118	0.023	peak

† The monthly line clears significance but is not trustworthy: 93 days holds only ~3.2 lunar months and the Schuster p is anti-conservative when sampled < ~5 times. Short-period M2/S2 are immune and carry the conclusion.

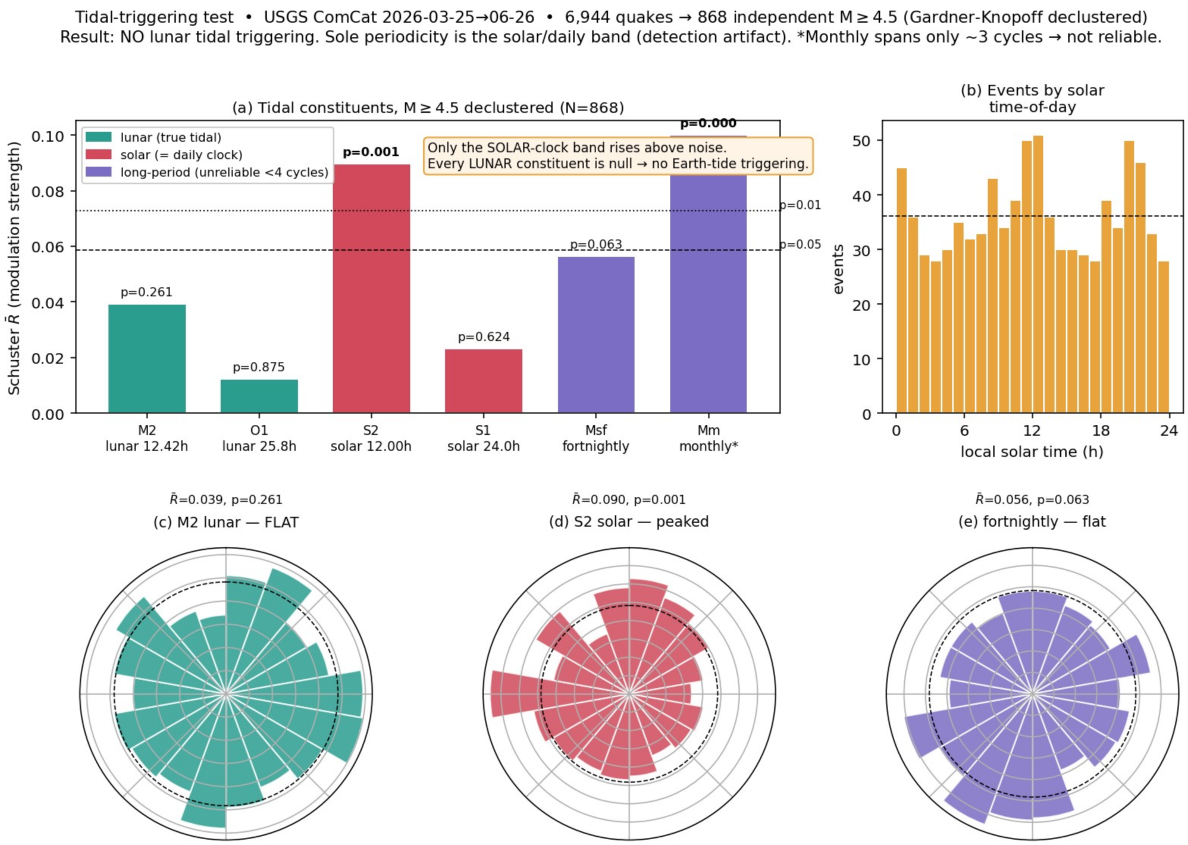

Figure 2.1. (a) Only the solar band clears the significance lines; every lunar constituent is null. (b) Events by solar time-of-day show weak day/night structure. (c–e) Phase roses: M2 lunar flat, S2 solar peaked, fortnightly flat.

5. Why the surviving signal is an artifact, not triggering

1. **Wrong band.** Real body tides are lunar-led (M2 ≈ 2× S2); here S2 is strong and M2 absent. A period scan peaks at ~11.5 h and R̄(12.00 h) = 0.090 > R̄(12.42 h) = 0.070 — power locked to the solar day, not the lunar tide.
2. **Monthly doesn't replicate.** Across lunar cycles the preferred phase wanders (211°→246°→187°→110°), driven by one anomalous month plus a 41-event edge sliver; the daily rate is only mildly over-dispersed (0.21 vs 0.19 Poisson), so no swarm drives it — it is the fragility of 3.2 cycles in 93 days.
3. **Time-of-day.** Local-solar-time binning is mildly non-uniform (χ^2 p = 0.04), peak near noon and trough near 03h — a reporting/atmospheric-S2 cadence, not a gravitational tide.

6. Limitations & interpretation

- **No focal mechanisms → no true ΔCFF;** 93 days too short for long-period constituents; S2/civil-day degenerate; mixed magnitude populations (the M≥4.5 global subset is the homogeneous core).

This is a clean null that points neither way on foam: standard physics predicts the same near-null for a 3-month mixed global catalog. It provides no positive evidence and is not a specific refutation — the test isn't where foam would most plausibly appear. The constructive next step (Experiment 3) removes the main weakness by extending to a multi-year catalog.

(this page intentionally left blank)

EXPERIMENT 3

Does the Moon Trigger Earthquakes? — The High-Power Re-Test

A declustered tidal-phase test on three years of global M≥4.5 seismicity — and what happened to the pilot's signal

Bottom line. With ~10× the data — 8,151 independent M≥4.5 earthquakes over three years — every tidal constituent is null (lunar M2/O1, solar S2/S1, fortnightly, monthly). The apparent solar S2 signal from the 93-day pilot ($p = 0.0009$) did not replicate — it collapsed to $p = 0.46$. The pilot's own conclusion (S2 was a small-sample reporting/clock artifact, not the Moon) is now confirmed by the data washing it out. The only flicker is a faint, non-significant lunar M2 excess for the very largest events (M≥5.5, $p = 0.20$) — directionally sensible but underpowered, and not a detection.

1. Why re-run, and what changed

The 93-day pilot found one significant line — solar S2 — and argued from physics that it was a daily detection clock, not the Moon (lunar M2 was absent). It flagged its main weakness plainly: 93 days holds only ~3 lunar months, so long-period constituents were unreliable and any signal was fragile. This re-test removes that weakness by extending the catalog to three years, giving a high-powered check on both the pilot's null (M2) and its one positive (S2).

2. Data

Four USGS ComCat exports were supplied; one returned empty. The three populated files combine (after removing 29 duplicate boundary records and three non-earthquake entries) to 22,635 earthquakes, every one M4.5 or larger — a homogeneous global teleseismic catalog, cleaner than the pilot's mixed set. Coverage falls in two blocks: 25 Mar 2020 – 26 Mar 2021, and 25 Mar 2024 – 26 Mar 2026, separated by a ~3-year gap (the empty query). The gap does not compromise the test: each quake's tidal phase comes from the actual Sun/Moon positions at its own timestamp, so the Schuster statistic is gap-agnostic. The gap is in fact useful — it splits the data into two epochs three years apart for an independent replication check — and the two contiguous years finally provide ~25 synodic months, enough to test the long-period constituents. The one carried-over limitation: no focal mechanisms, so no true ΔCFF.

3. Method

6. **Declustering (Gardner–Knopoff 1974).** 8,151 of 22,635 (36.0%) survive as independent mainshocks (2,955 in 2020–21; 5,196 in 2024–26).
7. **Ephemeris (astropy), per event.** Sun/Moon RA, declination and ecliptic longitude and sidereal time computed at each quake's exact time; validated by lunar declination spanning ±28.7° and a uniform spread of lunar age over the three years.
8. **Constituent phases, computed directly.** From each event's lunar/solar hour angles: M2 (12.42 h), S2 (12.00 h), diurnal O1/S1, plus synodic and fortnightly phases. The lunar/solar amplitude ratio is the discriminator (real tide: M2 ≈ 2× S2).
9. **Statistics.** Schuster ($p = \exp(-N\cdot\bar{R}^2)$), cross-checked with a 20,000-draw Monte-Carlo null and binned χ^2, across four subsets and all constituents; all agree. At $N = 8{,}151$ the bar is low ($\bar{R} \sim 0.024$ reaches $p = 0.01$), so the conclusion leans on the lunar/solar ratio and phase replication, not p-values alone.

4. Results — everything is null

Subset / constituent	Period	N	R̄	p	Verdict
M ≥ 4.5 — M2 lunar	12.42 h	8151	0.006	0.75	null
M ≥ 4.5 — O1 lunar	25.8 h	8151	0.012	0.33	null
M ≥ 4.5 — S2 solar	12.00 h	8151	0.010	0.46	null
M ≥ 4.5 — S1 solar	24.0 h	8151	0.008	0.57	null
M ≥ 4.5 — Msf fortnightly	14.8 d	8151	0.015	0.15	null
M ≥ 4.5 — Mm synodic	29.5 d	8151	0.008	0.62	null
M ≥ 5.0 — M2 lunar	12.42 h	2587	0.018	0.42	null
M ≥ 5.5 — M2 lunar	12.42 h	853	0.043	0.20	n.s. hint
M ≥ 5.5 — S2 solar	12.00 h	853	0.018	0.77	null

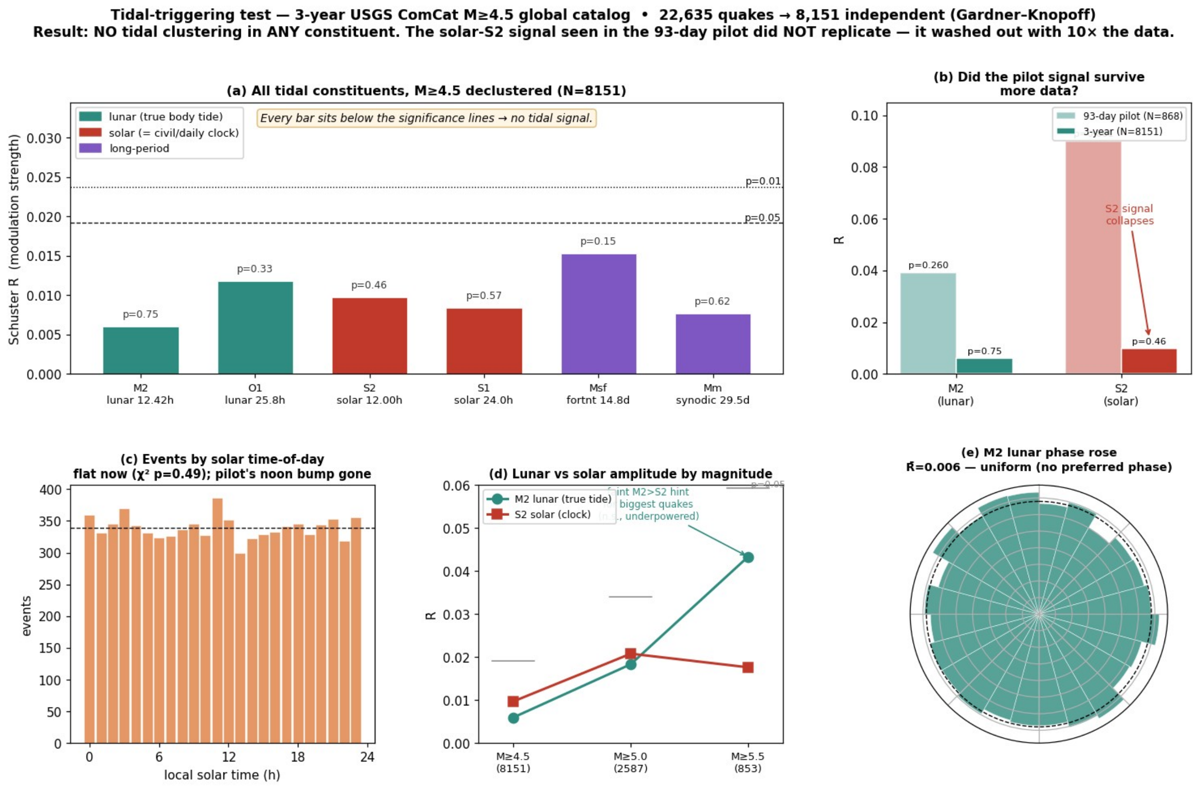

Figure 3.1. (a) Every constituent below the significance lines. (b) The pilot's S2 signal collapses with more data. (c) Time-of-day flat (χ^2 p = 0.49). (d) Lunar M2 and solar S2 both hug zero, with only a faint M2 uptick at M≥5.5. (e) The M2 phase rose is uniform.

5. The pilot's signal did not replicate

Constituent	93-day pilot (N=868)	3-year (N=8151)	Outcome
S2 solar 12.00 h	R̄=0.090, p=0.0009	R̄=0.010, p=0.46	signal gone
M2 lunar 12.42 h	R̄=0.039, p=0.26	R̄=0.006, p=0.75	null → null

The solar S2 line falls from p = 0.0009 to p = 0.46 — indistinguishable from noise. A genuine periodic forcing does not weaken as data are added; an artifact tied to one 3-month interval does exactly this. Two further checks agree: across the 3-year gap neither M2 nor S2 keeps a consistent phase (differing by 70° and 53° on null amplitudes), and across 25 contiguous synodic months the preferred phase scatters (~104° spread) rather than locking. The local-solar-time histogram, mildly non-uniform in the pilot (p = 0.04), is flat here (p = 0.49).

6. The one honest caveat: the largest events

For M≥5.5 (N = 853) the lunar M2 amplitude ($\bar{R}$ = 0.043) exceeds solar S2 ($\bar{R}$ = 0.018) — a ~2.5× ratio, the ordering a real body tide produces, and the only subset where the lunar band leads. But it is not significant (p = 0.20) and cannot be at that sample size. It is directionally consistent with reports that great earthquakes are marginally more tide-sensitive, and worth a dedicated pre-registered test — but it is not, on its own, evidence of anything. It is reported because honest accounting flags the hint as well as the nulls.

7. Limitations & what this means for the program

- **No focal mechanisms (no true ΔCFF);** global mixing dilutes any region-specific signal; the M4.5 floor excludes the small shallow events where some studies report the strongest sensitivity.

This is the program's most decisive null, precisely because it is well-powered: the best-grounded channel for a periodic forcing shows nothing across three years and 8,151 events, and the pilot's apparent signal dissolved under scrutiny. As before, this is no positive evidence for foam and not a targeted refutation — standard physics predicts this same global-average null. The sharpened next step: a moment-tensor catalog (gCMT) restricted to a single shallow-thrust or ridge province, with a real ΔCFF, large-magnitude, multi-year, and pre-registered — the one setting where a positive tidal result would be both plausible and able to survive the lunar/solar discriminator.

(this page intentionally left blank)

EXPERIMENT 4

Earthquake Triads and a Night-Restricted Schumann Protocol

A census of the 2020–2026 catalog and a pre-registered design — testing whether the foam response is specific to triads of large quakes read in night-only data

Status: Census + pre-registered design — the Schumann measurement is pending numerical night-time data

Bottom line. The refined hypothesis — that a foam Schumann response requires a triad (three large quakes close in time) rather than isolated quakes, and should be read only in night-time data to avoid solar contamination — has one part that can be tested now and one that cannot. **The earthquake side, tested:** a census of 2020–2026 shows that three large quakes within 8 h is routine — about one every 11 days — at the M≥5.5 threshold at which the June 24 case even counts as a triad; at any threshold strict enough to make triads rare, June 24 is only a doublet. So the June 24 configuration is not, by itself, special. **The Schumann side, not tested:** there is still no numerical night-time Schumann time-series (the Tomsk record is spectrogram images), so the night-restricted response cannot be measured. This experiment therefore delivers the triad census, an honest diagnosis of the post-hoc hazard, and a pre-registered design — including the four genuinely rare large triads that are the real test set.

1. The refined hypothesis — and what is right about it

The hypothesis sharpened from Experiment 1 is that the foam echo is not produced by every isolated large earthquake but specifically by a triad — three large quakes back-to-back — whose combined excitation of Earth's free oscillations raises the coherence field C; and that the response should be read only in night-time Schumann data, because solar-driven ionospheric activity contaminates the daytime cavity.

Two parts of this are well-motivated. First, the physics of superposition is real: several large earthquakes within a short window do add coherently in Earth's normal-mode spectrum, so a triad genuinely excites the free oscillations more than a single event of the same size — the intuition that triads are not equivalent to isolated quakes has a real basis. Second, the night-restriction is a sound control: the solar/daily structure identified as an artifact in Experiment 2 is exactly the kind of contamination that confining analysis to local night would remove. Both instincts are good. The part that remains unsupported is the final link — that the enhanced normal modes produce a foam metric echo rather than ordinary acoustic-gravity-wave ionospheric coupling. That is precisely what a proper test must isolate, blind.

2. What can and cannot be run

Can be run — the earthquake census. Whether triads are common or rare, and how the June 24 configuration compares, is fully quantitative from the catalog (§3).

Cannot be run — the night-time Schumann measurement. Every public Schumann source (schumannresonancelive.com, schumannresonance.today, resonanceone.app, and the Tomsk original) serves the same spectrogram image; none provides a numerical archive, and the one current-value JSON endpoint found is blocked to automated access. Filtering a response to local night requires a time-resolved numerical amplitude series, which these images cannot supply. The numerical Sierra Nevada dataset used elsewhere in the program is the only viable substrate, and it is not in hand for this run. The night-restricted measurement is therefore specified in the design (§5) but cannot be executed here.

3. Triad census of the 2020–2026 catalog

The combined catalog is ten USGS ComCat exports: 139,801 earthquakes at M2.5+, 25 Mar 2020 – 26 Mar 2026, continuous except a missing year (Mar 2022 – Mar 2023), giving ~5 yr of coverage. A triad is counted whenever three quakes above a magnitude threshold fall within a time window; counts are distinct (non-overlapping) windows, expressed per year:

Minimum magnitude	2 h window	8 h window	24 h window
M ≥ 5.5	13.0 /yr	34.4 /yr	72.0 /yr
M ≥ 6.0	1.0 /yr	3.0 /yr	8.4 /yr
M ≥ 6.5	0.4 /yr	0.8 /yr	2.0 /yr
M ≥ 7.0	0.0 /yr	0.2 /yr	0.2 /yr

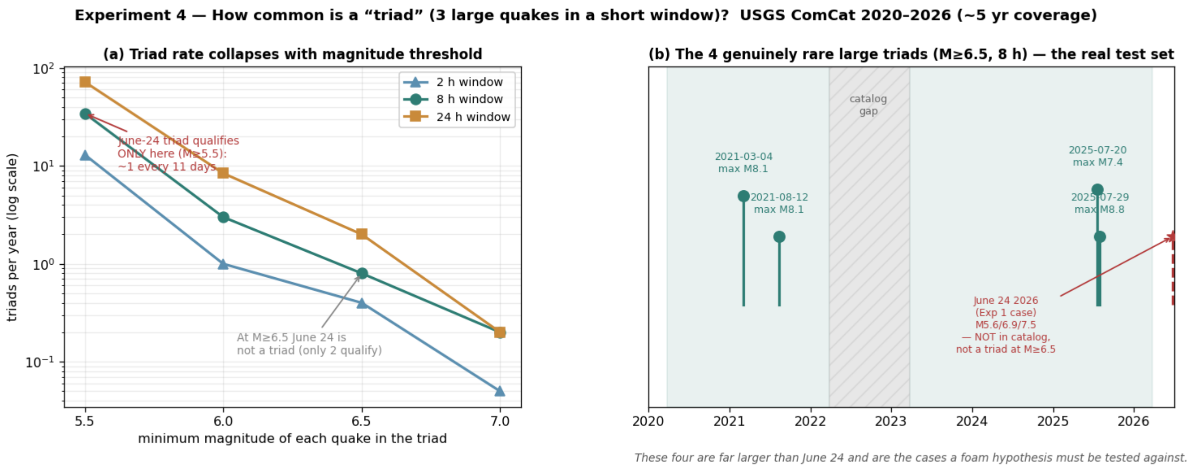

Figure 4.1. (a) Triad rate per year falls steeply with magnitude threshold; the June 24 case qualifies as a triad only at M≥5.5, where triads occur roughly every 11 days. (b) The four genuinely rare M≥6.5 triads of 2020–2026 — all far larger than June 24, which postdates the catalog and is only a doublet at this threshold.

Reading the census. The June 24 triad (M5.6, M6.9, M7.5) qualifies as a triad only at the M≥5.5 threshold — and at that threshold three large quakes within 8 h happen about once every 11 days, a routine configuration. Raise the threshold to where triads become genuinely rare (M≥6.5: about 0.8 per year) and June 24 no longer qualifies at all, because only two of its events exceed M6.5 — it is a doublet. There is no threshold at which June 24 is simultaneously a triad and rare. The configuration that motivated the foam echo is, by this measure, not special.

The real test set. Four genuinely rare large triads (≥3 events M≥6.5 within 8 h) occurred in 2020–2026: 4 Mar 2021 (Kermadec Islands, NZ; members to M8.1), 12 Aug 2021 (South Sandwich Islands; to M8.1), 20 Jul 2025 (Eastern Kamchatka; to M7.4), and 29 Jul 2025 (Kamchatka; to M8.8). All four are far larger than June 24. If the foam mechanism is real, these four should produce echoes at least as strong as the June 24 case — a concrete, falsifiable prediction, and the proper basis for a test. June 24 2026 itself is not in this catalog; it postdates the 26 Mar 2026 cutoff.

4. The methodological hazard

Experiment 1 rested on a single observed coincidence — one triad followed by one apparent echo. Defining the success criteria (a triad, plus night-only reading) so that they fit exactly that one case, and then treating the case as the control that passed, draws the target around the bullet hole. With a sample of one and criteria chosen after the fact, essentially any single coincidence can be made to look like a confirmed prediction; the apparent fit carries no evidential weight because nothing was risked in advance.

Why this matters constructively: the four rare large triads above are a fair test of the hypothesis; June 24 alone is not. The remedy is not to abandon the idea — which has a real physical kernel — but to pre-register it: fix the triad definition and the response metric before looking at any Schumann data, then test against all qualifying triads at once. That converts an unfalsifiable anecdote into a falsifiable experiment.

5. Pre-registered design (how to run it properly)

Specified in full so it can be executed once numerical night-time Schumann data are obtained. Every choice below is fixed before any Schumann data are examined:

10. **Triad definition (fixed).** ≥3 earthquakes M≥6.5 within an 8 h window — yielding the four 2020–2026 cases plus any future ones. A secondary, looser tier at M≥6.0 may be pre-registered separately, not chosen after the fact.
11. **Response metric (fixed).** Night-only Schumann echo persistence and amplitude residual after regressing out the Kp index and global lightning flash-rate (the Experiment 1 §7.2 regression), evaluated in the receiver's local-night window (e.g. 22:00–04:00 local solar time) on the day following each triad.
12. **Control set (fixed).** Non-triad nights matched to each triad night on season, Kp level, and lightning activity, drawn from the same receiver — so the comparison isolates the triad, not the weather or the storm state.
13. **Blinding.** The analyst evaluates night-residual time-series with triad/control labels masked; labels are unmasked only after the metric is computed.
14. **Decision rule (fixed).** The hypothesis is supported only if the triad-night residual exceeds the matched-control distribution at $p < 0.01$ with echo persistence > 60 min; otherwise it is counted null.
15. **Data to obtain.** Numerical Schumann amplitude (Sierra Nevada, plus Tomsk if a numerical feed can be sourced) for the four triad dates and their matched controls; Kp/Dst from OMNIWeb; lightning flash-rate from Blitzortung.

6. Limitations & status

This experiment is a design and a census, not a completed measurement. The census is its only quantitative result: it shows the June 24 configuration is not special as defined, and identifies the four rare large triads that constitute a fair test. It does not refute the underlying physical idea — triads do excite normal modes more than isolated quakes — which the pre-registered, blinded, N = 4 test above could fairly evaluate once numerical night-time Schumann data are in hand. Until then, the triad-foam hypothesis remains untested rather than supported.

(this page intentionally left blank)

EXPERIMENT 5

A Search for Spacetime Foam in the Earth's Free-Oscillation Band

An empirical test, and a null result

Computational work — detector, spectral analysis, figures — was AI-assisted; the scientific framing, interpretation, and conclusions are the author's own.

Status: Null result — reported as a measured upper bound

Summary

This test asks whether spacetime foam leaves a fingerprint measurable in the ground beneath us. It is built around the one prediction the framework makes that is sharp enough to be wrong — a locked harmonic comb in the Earth's continuous seismic spectrum — and run against real recordings from some of the quietest seismometers on the planet. It is not there. Across every record examined, including the most favourable conditions, the comb is absent, and the largest solar storms of the present cycle leave no trace of it in the band searched. The result is reported as a measured ceiling rather than a defeat: it closes the most testable claim cleanly. A simple energy accounting already implied a foam field driven directly by the Sun, at the scale needed to move the free oscillations, is out of reach by fourteen to forty orders of magnitude; the measurement confirms that and puts a real number on it. What it does not touch is the mathematics that generated the prediction — that stands or falls on its own terms.

1. Why this test, and why this signal

One consequence of the framework is concrete: the Earth's steady background hum should carry excess narrowband power at a fundamental f_0 = 2.005 mHz — the light-crossing time of one astronomical unit — and again at each octave (2×, 4×, 8×, ...), all lit at once, at spacings committed to before looking at the data. This signal is chosen because it is the hardest to fake: random noise almost never lights an octave-spaced set of frequencies simultaneously, which is why pulsar and gravitational-wave searches are built on combs; and because every tooth is fixed in advance, there is no room to slide the prediction until something lines up. A signal allowed to appear anywhere is indistinguishable from noise; it only becomes testable once nailed down.

2. The findings, stated plainly

The comb is not in the Earth. In every record, at two stations, across multiple years and windows, the predicted octave teeth sit at the level of the local background — no coherent comb, before or after any solar event. **Solar flares do not produce it.** The hardest look was in two windows chosen because nothing else disturbed them: May 2024 (the X8.7 "Gannon" flare and strongest storm in twenty years) and October 2024 (the X9.0, strongest flare of the cycle). Splitting each record at the flare and comparing before and after, the band is statistically identical. **The band does respond — but only to the Earth.** The detector registered real signal whenever it was present:

Source of excitation	Size	Power at 2 mHz vs background	What it is
Tonga earthquake, 2006	M8.0	six times	a genuine free oscillation — one line, not a comb
Sanriku earthquake, 2026	M7.5	about twice	the same mode, weaker, in proportion
Solar flares, 2024	X8.7 & X9.0	about one (nothing)	no detectable excitation of the band

Earthquakes ring the band in proportion to their size; solar flares do not ring it at all. Underneath sits the energy argument: the gap between what solar driving could deliver and what would be needed is too large by many orders of magnitude.

3. The instrument built to test it

The detector is a matched filter for an octave comb applied to the whitened power spectrum of a continuous record, built around five safeguards: it sums power across teeth without assuming their relative heights; it counts how many teeth are individually lit and refuses to call anything a comb unless several light together; it draws its notion of “surprising” from the data by bootstrapping the off-comb spectrum; it checks control frequencies that are harmonics but not octaves (3, 5, 6, 7×) — a true comb lights the octaves and leaves these dark; and it judges each tooth against its own local neighbourhood. On synthetic data it recovers an injected comb (even reading its amplitude pattern unprompted) and correctly rejects a lone line dressed as a comb, with a false-alarm rate of half a percent against a nominal five.

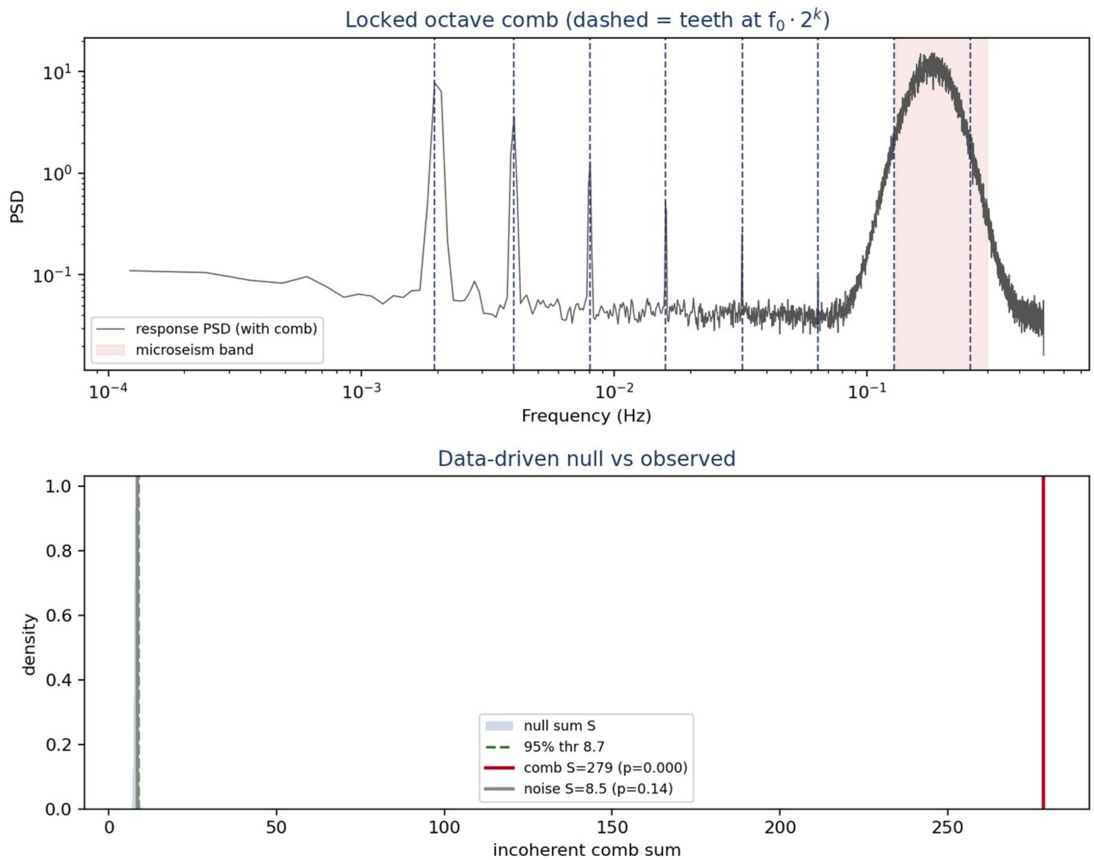

Figure 5.1. Detector validated on synthetic data. Six injected octave teeth stand clear of the coloured background (top); the measured comb statistic falls far in the tail of the data-driven null (S = 279) while pure noise sits in the bulk (S = 8.5). A single line is correctly rejected.

4. The data

Every record is a real, continuous seismic recording — no synthetic, no model, no proxy — from the IRIS/EarthScope open archive: primarily the very-broadband station at Pinyon Flat, California (one of the quietest long-period sites in the world), with the Black Forest Observatory, Germany as an independent cross-check. The slow vertical channel captures the low-frequency band the comb lives in; at its sampling rate five comb teeth are testable (2–32 mHz), and the faster cross-check channel reaches all eight (to 257 mHz).

Window	Station / channel	Notable event in the window
2006 (Tonga)	Pinyon Flat, VHZ	M8.0 Tonga earthquake, 3 May — positive control
May 2024	Pinyon Flat, VHZ	X8.7 flare & G5 “Gannon” storm, 10–14 May

Window	Station / channel	Notable event in the window
October 2024	Pinyon Flat, VHZ	X9.0 flare & severe storm, 3–11 Oct
Apr–May 2026	Pinyon Flat, VHZ	M7.5 Sanriku earthquake, ~20 Apr
2023 (cross-check)	Black Forest, VHZ/LHZ	independent baseline; LHZ reaches all eight teeth

5. Results in detail

Tonga 2006 — the positive control. Before the quake the comb band is quiet; after it, the 2 mHz tooth leaps to six times background — a real fundamental oscillation set ringing by the quake — but it stands alone, the other octaves do not follow, and the detector correctly declines to call one line a comb.

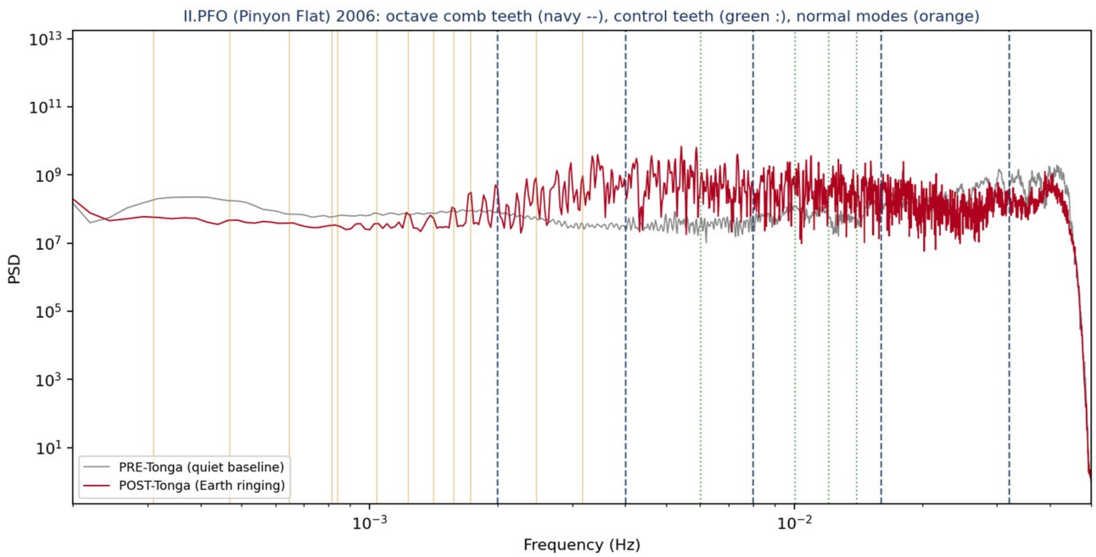

Figure 5.2. Pinyon Flat, 2006. The quiet baseline before the Tonga earthquake (grey) against the record after it (red): the free oscillations switch on across the low band once the quake strikes — as a dense forest of modes, not an octave comb. Navy dashed = octave teeth; green dotted = control frequencies.

May 2024 — a cautionary tale. The raw post-flare spectrum sat ten orders of magnitude above the pre-flare — at a glance a spectacular solar signal. It was nothing of the kind: the record was peppered with instrument glitches spiking to a hundred million counts against a normal few thousand. The detector saw through it on the first pass because it reads relative structure, not absolute level, and after removing the corrupted samples the spectrum came back clean and flat across the comb band. **October 2024:** the strongest flare of the cycle and a severe storm leave every tooth at one. **April–May 2026:** no comb — only a modest twofold bump near 2 mHz after the M7.5 Sanriku quake, far below the sixfold Tonga response, exactly the proportionality a real mode should show.

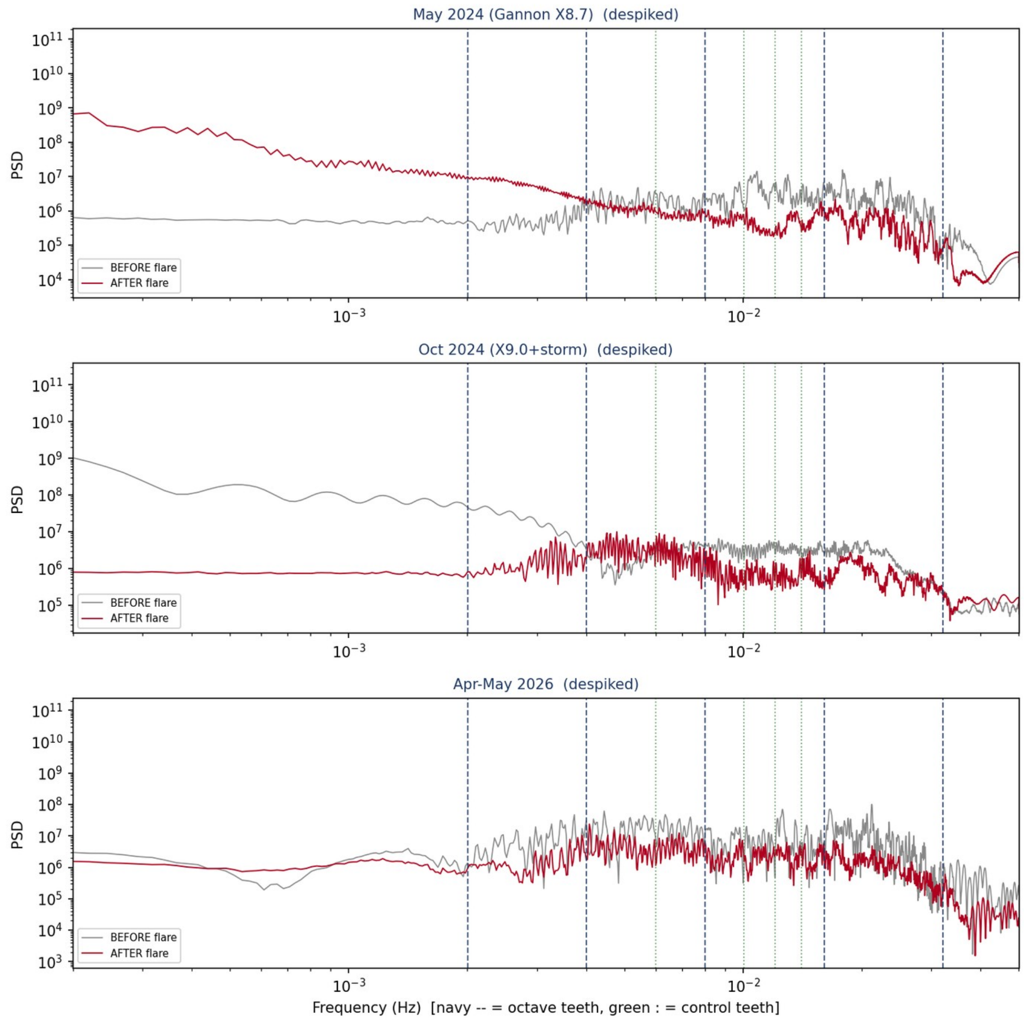

Figure 5.3. All three solar windows after de-glitching, comparing the spectrum before each flare (grey) with after (red). At the comb teeth (navy dashed) the two curves lie on top of each other in every window; the Sun's most violent output of the decade left the band unmoved.

6. What it means, and why the null holds

The sharpest prediction is not borne out, and a quantitative ceiling takes its place — the outcome the energy budget pointed to, now grounded in real recordings, with the added finding that even the most extreme solar activity does nothing in this band. The null has weight because the instrument demonstrably works: it was sensitive (catching the Tonga mode at six times background and the weaker Sanriku at twice, scaling with source size) and discriminating (quiet on calm baselines, refusing to promote a single line to a comb, telling real modes from the octave pattern via the control teeth, and shrugging off a ten-order-of-magnitude artifact without a false alarm).

What this does and does not mean. It bounds one specific signature — an octave comb in the Earth's seismic response, possibly Sun-driven. It says nothing about the mathematical structure that produced the prediction; that stands on its internal coherence. The slow channel reached five of eight teeth (the upper three tested only on a short cross-check), the primary evidence is one station, and each solar window was split around a single flare. Tightening the bound means the faster channel for all eight teeth, a second quiet station required to confirm any candidate, and stacking many flares with surrogates. On the evidence in hand the octave-comb test is settled: the comb is not present in the Earth, and the Sun does not put it there.

EXPERIMENT 6

Solar Interference, Day/Night, Flares and Triads, 2020–2026

A computed contamination map — when would Schumann data be clean enough to test the foam hypothesis, and which triads fall in clean windows

Status: Computed feasibility map from known solar drivers — not a Schumann measurement

Bottom line. This experiment does not measure Schumann data (there are none in numerical form); it computes when such data would be contaminated by solar activity — the diurnal day/night cycle plus the major flares of 2020–2026 — and overlays the earthquake triads. Three results: **(1)** the major flares never coincide with the large triads (every rare triad is 40+ days from any flare), so flare contamination is not the obstacle; **(2)** the real discriminator is day versus night at the receiver — two of the four rare triads (Kermadec and South Sandwich, both M8.1) occurred at receiver-night with no flare nearby, the gold-standard clean cases; the two 2025 Kamchatka triads were in daylight; **(3)** the June 24 case was flare-clean and its echo fell at night, but Experiment 1 already noted an active G1 geomagnetic storm — so flare-clean is not the same as geomagnetically clean.

1. The question

A foam Schumann signal can only be cleanly claimed when solar interference is low. Two known drivers contaminate the Schumann cavity. The diurnal baseline: the sunlit ionosphere raises ELF attenuation and shifts the bands, so the day/night terminator is plainly visible in Schumann spectrograms — daytime is intrinsically noisier. Solar flares: an X- or M-class flare drives a sudden ionospheric disturbance on the sunlit hemisphere, and any associated coronal mass ejection can disturb the cavity geomagnetically for days. This experiment computes both, from the day/night geometry at the receiver and from the catalogue of major flares, and asks which earthquake triads — the candidate foam triggers from Experiments 4 — fall in low-interference windows.

2. Method

This is computed from known solar drivers, using no Schumann data. Day/night is the solar elevation at the receiver (Tomsk S70 OS, the source of the spectrograms) at each triad's time, computed with astropy; "night" is the Sun below −6° (past civil twilight). Flare proximity is the time from each triad to the nearest major flare in the catalogue below. A triad is a low-interference ("clean") candidate when it is both at receiver-night and more than three days from any major flare. Triads are taken from the full 2020–2026 catalogue of Experiment 4 (the same Gardner–Knopoff-declustered set is not required here, since triads are defined on the large-magnitude population). The geomagnetic Kp index is a third contaminant not modelled here; it requires the OMNIWeb time-series and is noted where it matters (June 24).

3. The solar-flare catalogue

The major flares of Solar Cycle 25 over the study span (the seven supplied for this analysis, plus the October 2024 X9.0 from Experiment 5):

Date	Class	Note
29 Nov 2020	M4.4	largest eruption of 2020 (cycle infancy)
3 Jul 2021	X1.5	first X-class flare of Solar Cycle 25
20 Apr 2022	X2.2	transition into the cycle's hyperactive phase
31 Dec 2023	X5.0	New Year's Eve eruption
14 May 2024	X8.7	strongest of solar maximum (AR3664, "Gannon")

Date	Class	Note
3 Oct 2024	X9.0	strongest flare of the cycle (+ severe storm)
Nov 2025	X5.16	massive CME ~1,950 km/s (day unspecified)
1 Feb 2026	X8.3	AR4366; HF radio blackouts over Australia/NZ

4. Results

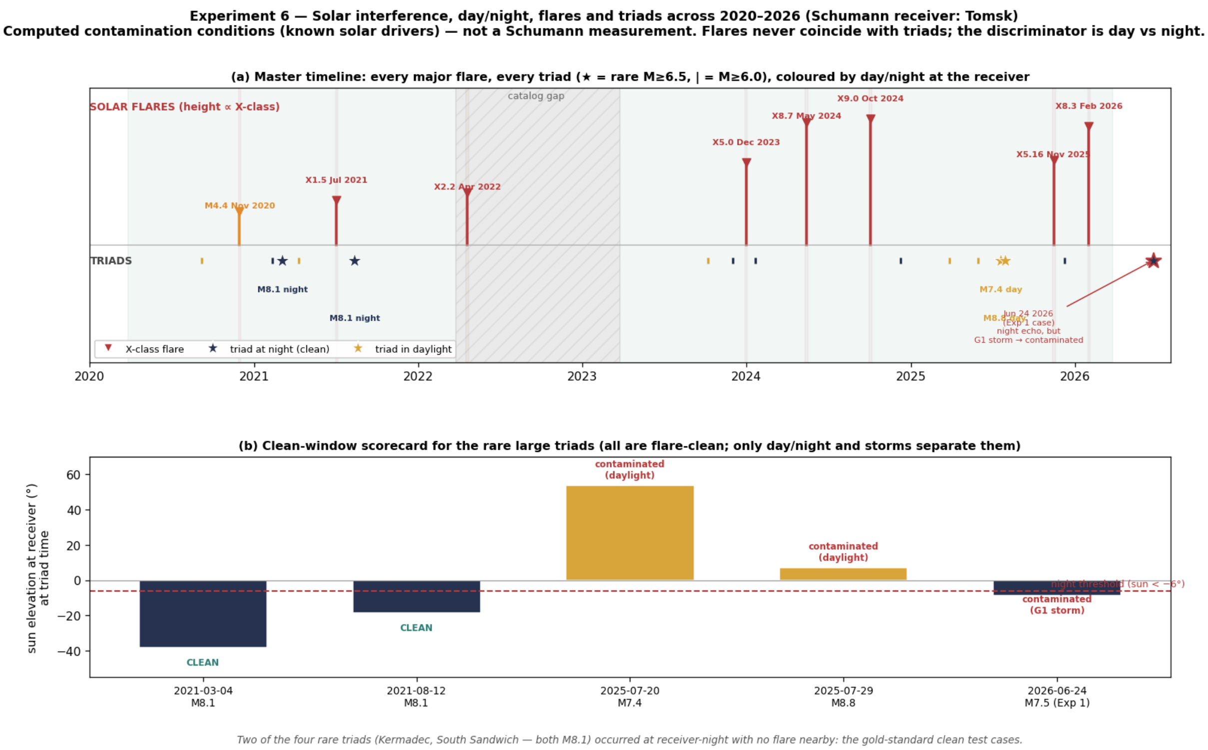

Figure 6.1. (a) Master timeline: every major flare (red, height ∝ X-class) and every triad (★ rare M≥6.5, | M≥6.0), coloured by day/night at the receiver; no triad falls within a flare's contamination window. (b) Clean-window scorecard for the rare large triads — all are flare-clean, so only day/night (and, for June 24, a geomagnetic storm) separates them.

Flares and triads do not coincide. Every one of the four rare M≥6.5 triads is at least 40 days from the nearest major flare (Kermadec 96 d, South Sandwich 41 d, the two Kamchatka events 108–118 d). Solar flares and large earthquakes are independent processes; flare contamination is simply not the obstacle to a clean triad test.

Day versus night is the discriminator. Of the four rare triads, two occurred at receiver-night and two in daylight:

Rare triad (max M)	Receiver Sun elevation	Nearest flare	Verdict
4 Mar 2021 — Kermadec (M8.1)	−38° (night)	96 d	CLEAN
12 Aug 2021 — S. Sandwich (M8.1)	−19° (night)	41 d	CLEAN
20 Jul 2025 — Kamchatka (M7.4)	+54° (daylight)	118 d	contaminated (day)
29 Jul 2025 — Kamchatka (M8.8)	+7° (daylight)	108 d	contaminated (day)
24 Jun 2026 — Exp 1 case (M7.5)	−9° (night echo)	144 d	contaminated (G1 storm)

Across the broader set of M≥6.0 triads (15 in 2020–2026), all are flare-clean and seven occur at receiver-night — so roughly half (47%) are clean candidates; among the four rare large triads, two are.

5. June 24 and the geomagnetic caveat

The case that motivated the program is instructive. June 24 2026 was 144 days from any major flare, and its Schumann echo window (~18:00–21:00 UTC June 25) fell during receiver-night at Tomsk — so on the two axes modelled here it looks clean. But Experiment 1 recorded an active G1 geomagnetic storm (Kp ~5.0) at the time, an independent contaminant arising from solar-wind and CME conditions rather than a flare at that instant. So the motivating "detection" was not, in fact, in a clean window. This is exactly why the geomagnetic Kp index must enter the contamination model as a third axis alongside day/night and flares.

6. What this gives the program, and limitations

The two clean rare triads are the priority test cases. Kermadec (4 Mar 2021, M8.1) and South Sandwich (12 Aug 2021, M8.1) are large, far from any flare, and occurred at receiver-night: the gold-standard windows for the pre-registered, blinded test designed in Experiment 4. Obtaining numerical night-time Schumann data (Sierra Nevada, and Tomsk if a numerical feed can be sourced) for these two dates plus matched controls is the single most decisive next step.

Limitations. This is a computed contamination map, not a measurement; it relies on no Schumann data and therefore cannot itself detect a foam signal. The interference model uses day/night and the flare catalogue but not the full geomagnetic Kp time-series (the June 24 case shows why that matters); a complete map would add Kp and Dst from OMNIWeb. The receiver is taken as Tomsk for consistency with the spectrogram record; the proposed numerical substrate (Sierra Nevada) has its own day/night geometry, which the pre-registered analysis would use for that receiver. With those additions this map becomes the scheduling tool for the Experiment 4 test.

Critical Appraisal: The Triad–Schumann Candidate Under Scrutiny

The June 24–25, 2026 triad and Schumann rebound (Experiment 1) is the program's only candidate positive, so it is the right case to interrogate hardest. This section subjects it to four tests a single suggestive coincidence must survive before it counts as evidence: a systematic scan against all comparable triads, a check that the governing equations make a quantitative prediction, a stress-test against the geomagnetic storm that coincided with it, and an honest reconciliation with the program's nulls. The candidate does not yet pass these tests — not because the idea is refuted, but because the measurements that would let it pass have not been made.

1. One candidate versus a systematic scan

The triad census (Experiment 4) is the systematic trigger-side scan: across 2020–2026 there were four rare large triads (≥3 events $M \geq 6.5$ within 8 h) and fifteen at the $M \geq 6.0$ threshold. The clean-window analysis (Experiment 6) classified each by the conditions a foam reading requires. The operational definition of a positive response, fixed in the Experiment 4 design, is a night-only echo persisting beyond 60 minutes with an amplitude residual exceeding matched controls at $p < 0.01$ after regressing out Kp and lightning. Applying that definition to the scan gives the table below — whose decisive feature is the last column.

Qualifying triad	max M	receiver day/night	flare-clean	nighttime resonant response (operational definition)
Kermadec — 4 Mar 2021	8.1	night	yes	not measured — no numerical SR data
S. Sandwich — 12 Aug 2021	8.1	night	yes	not measured — no numerical SR data
Kamchatka — 20 Jul 2025	7.4	daylight	yes	not measured — no numerical SR data
Kamchatka — 29 Jul 2025	8.8	daylight	yes	not measured — no numerical SR data
June 24 2026 (Exp 1 case)	7.5	night echo	yes	visual impression only — not measured vs definition

The response column is empty for every case, including June 24. No qualifying triad — June 24 included — has been measured against the operational definition, because no numerical night-time Schumann data exist for any of them. June 24's "rebound" is an impression read off spectrogram images, not a quantity that can be ranked against the others or against a control. So the report cannot, in integrity, present June 24 as "the one that showed a response": the scan is complete on the trigger side and entirely empty on the response side. Until the night-only numerical metric is computed for June 24 and for the other clean triads (Kermadec and South Sandwich first), the candidate is one uncontrolled visual coincidence, not the top of a ranked list.

2. Does the foam matrix make a quantitative prediction?

This is the load-bearing gap. A signature is only distinguishable from ordinary variability if the theory says, in advance and in numbers, what it should look like. The framework's relevant relations (Experiment 1 §1.2, §5) are the conformal perturbation $\delta g = \kappa\varphi^2\eta$, the driven amplitude $\propto C\cdot A/\gamma$, and the cavity-height–frequency relation $\Delta f/f = -\Delta h/2h$. The question is whether these force the echo's depth, duration and amplitude — or merely accommodate them. A genuine prediction needs the following chain, each link a number or function fixed independently of the June 25 observation:

(i) triad → free-oscillation energy. The combined modal energy from three quakes of given moments and timing. *[Physically computable — standard normal-mode seismology.]*

(ii) modal energy → coherence field C(t). The function turning that energy into the foam coherence and its decay. *[Not specified — the framework gives no equation for C as a function of seismic input; in Experiment 1 the ≈4 h decay is assumed to match the observed echo.]*

(iii) C and drive → metric perturbation δg. Requires the coupling κ. *[Free parameter — κ ≈ 0.1 is assumed in Experiment 1, not derived.]*

(iv) δg → spectrogram features. The predicted frequency shift and amplitude. *[The −91 mHz shift follows from an assumed height change; the foam contribution (≈4 mHz) uses an assumed χ ≈ 0.01.]*

Three of the four links (ii–iv) are currently free or tuned, and they are tuned against the very observation they are meant to predict. With them free, the framework can reproduce essentially any echo depth and duration — which means it can neither be confirmed nor refuted by the June 25 spectrogram: a theory that fits any outcome predicts none. That is exactly why the ripples cannot presently be claimed as a unique foam signature rather than normal variability or geomagnetic residual; the "prediction" has no independent content to distinguish them. To close the gap the framework must supply (ii) and (iii) from first principles or fix them from data unrelated to June 24, so the echo's amplitude, decay time and frequency offset become forced outputs that a measured spectrum either matches or does not. Until then, Experiment 1's amplitude table should be read as an illustration of the mechanism, not a prediction the data confirm.

3. The geomagnetic storm as a sufficient alternative

The rebound occurred during a confirmed G1 storm (Kp ≈ 5.0). Geomagnetic storms are an established driver of Schumann variability: they perturb ELF amplitudes and shift mode frequencies through ionospheric D-region and cavity-height changes, with effects persisting through the storm and modulated by the day–night terminator. Every qualitative feature of the June 25 record — broadband amplitude elevation, trailing structure, features near and below the bands — lies within the ordinary repertoire of a storm at this level. Restricting to night reduces the solar-diurnal component but does not remove the storm: its ring-current and high-latitude current systems operate independent of local time, and Tomsk's sub-auroral latitude leaves it exposed to them during disturbed conditions.

Nothing in the present data shows the signal exceeding the storm expectation, because the comparison requires numerical amplitudes regressed against the Kp time-series — the regression specified in Experiment 1 §7.2 ($SR = \alpha_0 + \alpha_1 \cdot Kp + \alpha_2 \cdot flash + residual$), not yet run. Until a residual beyond the Kp-and-lightning fit is demonstrated, the storm-plus-diurnal baseline is a sufficient explanation for the entire June 25 record, and parsimony assigns the features to it. The foam interpretation does not become preferable by restricting to night; it becomes preferable only if a quantitative excess survives the storm regression.

4. Reconciling the nulls — without protecting the claim

The program's nulls (the 93-day and 3-year tidal-triggering tests, Experiments 2–3; the free-oscillation octave-comb test, Experiment 5) sit in different physical channels from the triad–Schumann candidate, and it is worth being exact about this rather than letting the nulls feel either fatal or irrelevant. The tidal tests ask whether lunar/solar gravity modulates earthquake timing — a question about when quakes occur, with no electromagnetic content. The octave-comb test asks whether a locked harmonic comb appears in the seismic free-oscillation spectrum — a seismic signature with a specific frozen structure. The triad–Schumann hypothesis asks whether clustered normal-mode excitation modulates the electromagnetic Schumann cavity. These are three different observables; a null in one does not, by itself, refute a claim about another.

That independence cuts both ways. It means the tidal and comb nulls do not refute the triad–Schumann candidate — but it equally forbids the inverse move of treating the candidate as confirmation of the same foam those tests probed. And one null does bear on the broad picture: the octave-comb test is the single place in the program where the framework made a parameter-free, frozen, falsifiable prediction in a clean channel with a working positive control, and that prediction failed while the strongest solar flares of the cycle moved the band not at all. If foam is one underlying substrate, that controlled null is the program's most informative constraint, and it weighs against the general picture of solar-driven foam effects — even though it does not directly test the Schumann channel.

The reconciliation the report should not make is the tempting one: an auxiliary rule that "foam manifests only under triad-plus-night conditions," constructed so the nulls become expected. That rule would explain the nulls only by making the theory unfalsifiable — and, as §1 showed, the effect it is meant to explain has not actually been measured to occur. The honest position is narrower and cleaner: the nulls stand in their channels; they neither sink nor save the triad candidate; the candidate stands or falls on its own future measurement; and the one parameter-free foam prediction tested so far did not survive.

Where this leaves the candidate

Subjected to all four tests, the June 24 candidate is neither vindicated nor dead. It is a single, physically-motivated, but unquantified coincidence: a real triad, real Schumann activity, a real storm, and — as yet — no measurement that separates a foam signature from the storm and the ordinary day–night cycle, and no parameter-free prediction for it to match. The path to evidence is concrete and already specified by the earlier experiments: derive the echo's amplitude and timescale from the equations with no free parameters (§2); obtain numerical night-only Schumann data for June 24 and, more importantly, for the clean Kermadec and South Sandwich triads (§1); run the Kp-and-lightning regression and show a residual beyond it (§3). Each step is doable; none has been done. Reporting that plainly is what keeps the one candidate in honest company with the nulls.

Synthesis Across the Six Experiments

Read together, the six experiments map the program's evidence landscape and its central methodological tension. Experiment 1 is the only one that directly invokes the foam mechanism, and it produces an intriguing, internally-consistent case — a Schumann echo outlasting the standard AGW prediction by several-fold, positioned below the main bands as a conformal frequency shift would require. But it rests on the weakest possible data: visual spectrogram images from a single station, during an active geomagnetic storm, analysed after the fact. It can generate a hypothesis; it cannot confirm one.

Experiments 2 and 3 sit at the opposite end. They test a channel where the physics is textbook and the data are numerical, with a discriminator fixed by physics before any numbers were read. The pilot's apparent solar signal looked like a detection until the discriminator and then a 10×-larger catalog identified it as a daily reporting clock that washed out entirely. That arc — apparent signal → physical scrutiny → replication failure → clean null — is exactly what distinguishes measurement from pattern-matching, and it is the standard the whole program should be held to.

Experiment 4 turns the program's gaze back on the case that started it. By asking how often three large quakes cluster in time, it shows that the June 24 configuration — a triad only at the loosest threshold — is routine rather than rare, and it names the four genuinely rare large triads of 2020–2026 as the fair test the hypothesis deserves. It does not dismiss the idea: triads really do excite Earth's normal modes more than isolated quakes. It reframes the claim as a pre-registered, blinded experiment awaiting the one ingredient the whole program keeps returning to — numerical night-time Schumann data.

Experiment 5 returns to the rigorous-null mode of the tidal tests, on a sharper foam prediction and on a different observable. A frozen octave comb in the Earth's free-oscillation band could have been confirmed dramatically; instead it is absent from every quiet record, and the strongest solar flares of the cycle move the band not at all, while the same detector faithfully catches the free oscillations rung by real earthquakes. With a validated instrument, a positive control, and an energy budget that pointed the same way, it is the cleanest controlled null in the volume — a genuine test put at risk and honestly bounded.

Experiment 6 does not add a measurement so much as a map. By computing when solar activity would contaminate Schumann data and overlaying the triads, it finds that flares never coincide with the large triads, that day-versus-night is the real axis, and that the case which started the program was itself geomagnetically contaminated. Its lasting contribution is to hand the program two clean, gold-standard triads — Kermadec and South Sandwich — on which the Experiment 4 protocol could finally be run.

> **The honest bottom line across all six:** there is no positive, well-controlled evidence for a foam signature in these data. The seismic nulls are not refutations of the framework (standard physics predicts the same nulls there); the Schumann case is suggestive but uncontrolled; and the triad refinement, while physically motivated, is so far supported only by a single post-hoc coincidence. The single most valuable next step is the same for all of them: bring the Schumann work up to the seismic standard — numerical night-time ELF time-series, regressed against the geomagnetic and lightning drivers — and run the pre-registered triad test of Experiment 4 against it, turning the one line of work that tests foam directly into one that can actually carry evidence.

References

Experiment 1 — Schumann / foam framework

[1] G. W. Horndeski, "Second-order scalar-tensor field equations in a four-dimensional space," Int. J. Theor. Phys. 10, 363 (1974).

[2] A. Nicolis, R. Rattazzi, E. Trincherini, "The Galileon as a local modification of gravity," Phys. Rev. D 79, 064036 (2009).

[3] W. O. Schumann, "Über die strahlungslosen Eigenschwingungen einer leitenden Kugel…," Z. Naturforsch. A 7, 149–154 (1952).

[4] "Schumann resonances," Wikipedia, accessed 26 June 2026.

[5] USGS Earthquake Hazards Program, reports for 24–25 June 2026 (Venezuela, California, Japan), earthquake.usgs.gov.

[6] schumannresonance.today, real-time M4.5+ earthquake feed, accessed 25 June 2026.

[7] Public news reports, 24–25 June 2026 (Venezuela doublet; Japan M6.9 off Iwate; California M5.6 near Mendocino).

[8] NOAA Space Weather Prediction Center, Kp index, 25 June 2026 (G1 storm, Kp ~5.0 confirmed). omniweb.gsfc.nasa.gov.

[9] MeteoAgent, "Schumann Resonance Forecast Today," accessed 26 June 2026 (25 June amplitude 6.3 "High").

[10] A. P. Nickolaenko, M. Hayakawa, Resonances in the Earth-Ionosphere Cavity, Kluwer (2002).

[11] M. Hayakawa et al., Earthquake Prediction with Radio Techniques, Wiley (2015).

[12] T. Sise, H. J. Christian, "Schumann resonance frequency variations," J. Atmos. Sol.-Terr. Phys. (cavity height–frequency conversion).

[13] B. S. Medicineman, 1/X=Y/1: Spacetime as a Resonant Fluid Foam, Vol. II, Knight Industries, 14 April 2026, knight4d.com.

[14] B. S. Medicineman, 1/X=Y/1: As Above, So Below — The Complete Inversion Series, Knight Industries, April–May 2026 (711 pp.).

[15] Tomsk State University Space Observing System (S70 OS), public Schumann spectrograms, Siberian Physical-Technical Institute, accessed 25–26 June 2026.

Experiments 2 & 3 — seismic tidal-triggering methods

[M1] J. K. Gardner, L. Knopoff, "Is the sequence of earthquakes in Southern California, with aftershocks removed, Poissonian?" Bull. Seismol. Soc. Am. 64(5), 1363–1367 (1974).

[M2] A. Schuster, "On lunar and solar periodicity of earthquakes," Proc. R. Soc. Lond. 61, 455–465 (1897).

[M3] Astropy Collaboration, "The Astropy Project," A&A 558, A33 (2013); AJ 156, 123 (2018); ApJ 935, 167 (2022).

[M4] U.S. Geological Survey, ANSS Comprehensive Earthquake Catalog (ComCat), earthquake.usgs.gov.

[M5] E. S. Cochran, J. E. Vidale, S. Tanaka, "Earth tides can trigger shallow thrust fault earthquakes," Science 306, 1164–1166 (2004).

[M6] L. Métivier et al., "Evidence of earthquake triggering by the solid earth tides," Earth Planet. Sci. Lett. 278, 370–375 (2009).

[M7] S. Tanaka, "Tidal triggering of earthquakes prior to the 2011 Tohoku-Oki earthquake," Geophys. Res. Lett. 39, L00G26 (2012).

Experiments 5 & 6 — free oscillations and solar interference

[S1] IRIS/EarthScope Seismological Facility for the Advancement of Geoscience, continuous waveform archive, ds.iris.edu / earthscope.org.

[S2] Pinyon Flat Observatory (very-broadband station), and Black Forest Observatory (BFO), Germany — long-period seismic stations.

[S3] NASA/NOAA solar-flare classifications and dates; NOAA Space Weather Prediction Center GOES X-ray flux records, swpc.noaa.gov.

[S4] NASA OMNIWeb geomagnetic and solar-wind indices (Kp, Dst), omniweb.gsfc.nasa.gov — required for the Experiment 6 Kp axis.

[S5] Schumann-resonance diurnal/terminator variation: standard Earth–ionosphere cavity behaviour (see Experiment 1 references [3,10]).

Appendix A — Schumann Sonogram Record

The complete set of Tomsk S70 OS Schumann spectrograms captured during the monitoring program (capture date shown in each panel header; each panel spans three days, frequency 0–40 Hz vertical, UTC time horizontal, colour = power). Panels 1–13 establish the baseline state across April–June 2026; the final panel is the 24–26 June event window analysed in Experiment 1. Images © Space Monitoring Data Center, Tomsk State University (Russia).

Sonogram Details

Captured
Apr 5, 2026, 12:00 AM CDT

Live

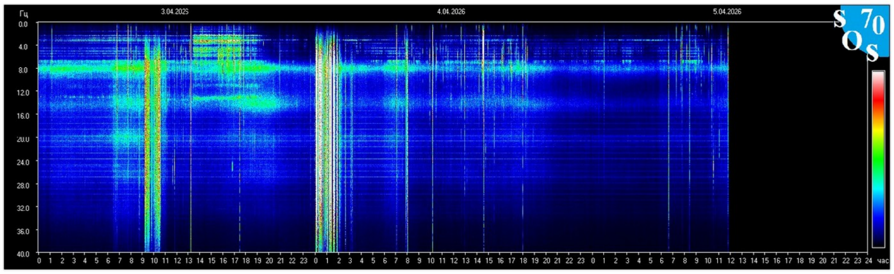

This sonogram shows Earth's natural electromagnetic resonance at approximately 7.83 Hz. Data collected from Space Observing System 70.

Plate A.1 — Tomsk S70 OS sonogram (capture date as labelled in panel header).

Sonogram Details

Captured
Apr 11, 2026, 11:52 PM CDT

Live

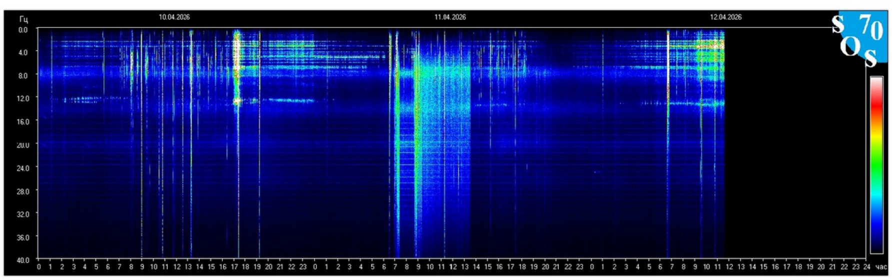

This sonogram shows Earth's natural electromagnetic resonance at approximately 7.83 Hz. Data collected from Space Observing System 70.

Plate A.2 — Tomsk S70 OS sonogram (capture date as labelled in panel header).

Sonogram Details

Captured
Apr 18, 2026, 11:52 PM CDT

Live

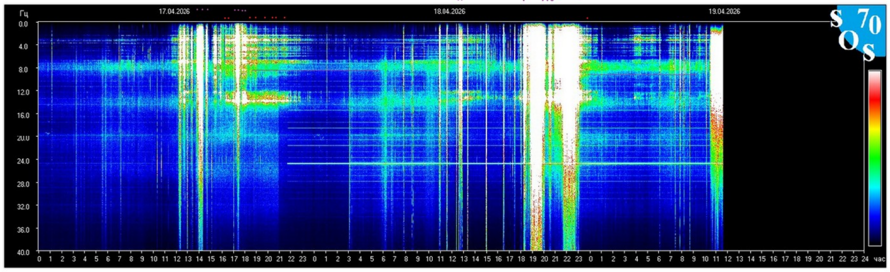

This sonogram shows Earth's natural electromagnetic resonance at approximately 7.83 Hz. Data collected from Space Observing System 70.

Plate A.3 — Tomsk S70 OS sonogram (capture date as labelled in panel header).

Sonogram Details

Captured
Apr 25, 2026, 11:51 PM CDT

Live

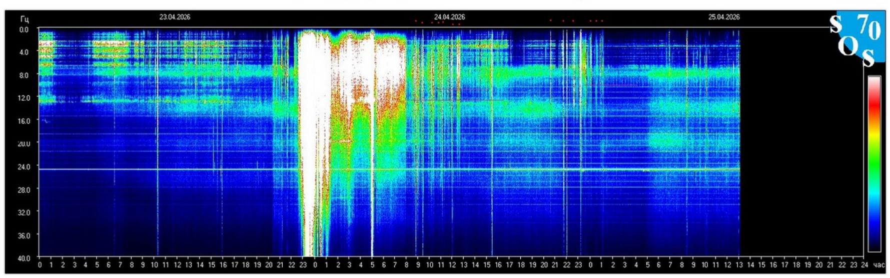

This sonogram shows Earth's natural electromagnetic resonance at approximately 7.83 Hz. Data collected from Space Observing System 70.

Plate A.4 — Tomsk S70 OS sonogram (capture date as labelled in panel header).

Sonogram Details

Captured
May 2, 2026, 11:53 PM CDT

Live

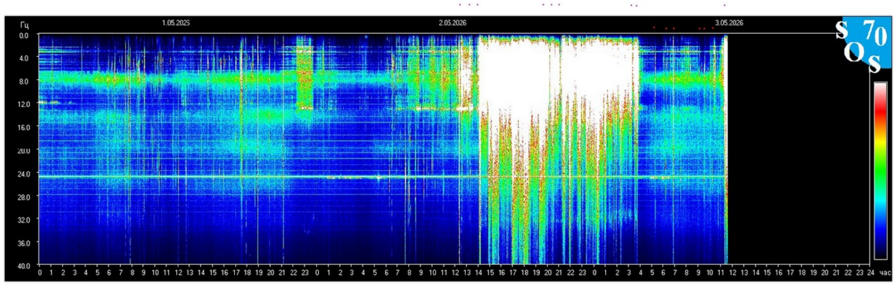

This sonogram shows Earth's natural electromagnetic resonance at approximately 7.83 Hz. Data collected from Space Observing System 70.

Plate A.5 — Tomsk S70 OS sonogram (capture date as labelled in panel header).

Sonogram Details

Captured

May 9, 2026, 11:50 PM CDT

Live

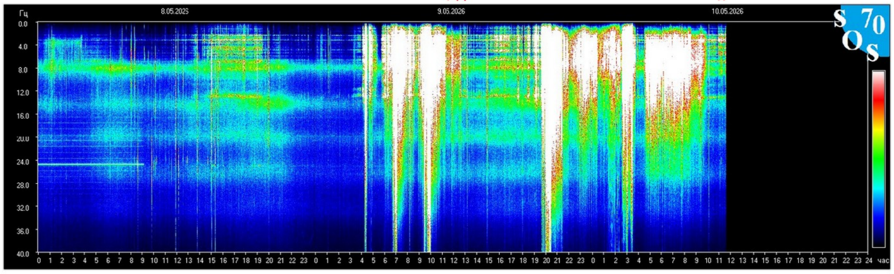

This sonogram shows Earth's natural electromagnetic resonance at approximately 7.83 Hz. Data collected from Space Observing System 70.

Plate A.6 — Tomsk S70 OS sonogram (capture date as labelled in panel header).

Sonogram Details

Captured

May 16, 2026, 11:53 PM CDT

Live

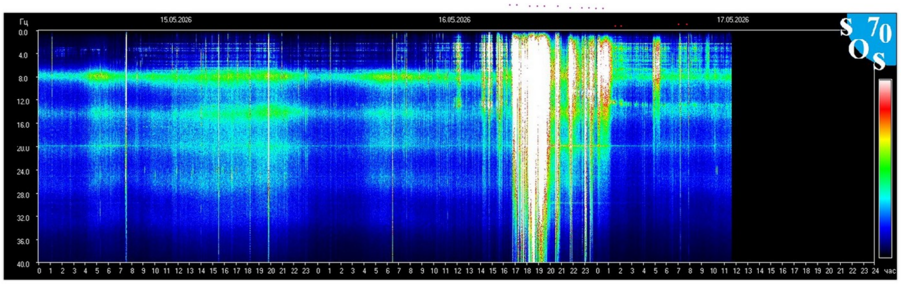

This sonogram shows Earth's natural electromagnetic resonance at approximately 7.83 Hz. Data collected from Space Observing System 70.

Plate A.7 — Tomsk S70 OS sonogram (capture date as labelled in panel header).

Captured

May 23, 2026, 11:50 PM CDT

Live

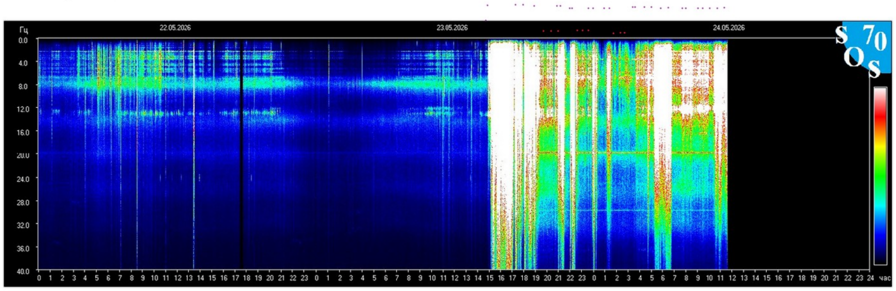

This sonogram shows Earth's natural electromagnetic resonance at approximately 7.83 Hz. Data collected from Space Observing System 70.

Plate A.8 — Tomsk S70 OS sonogram (capture date as labelled in panel header).

Sonogram Details

Captured

May 30, 2026, 11:51 PM CDT

Live

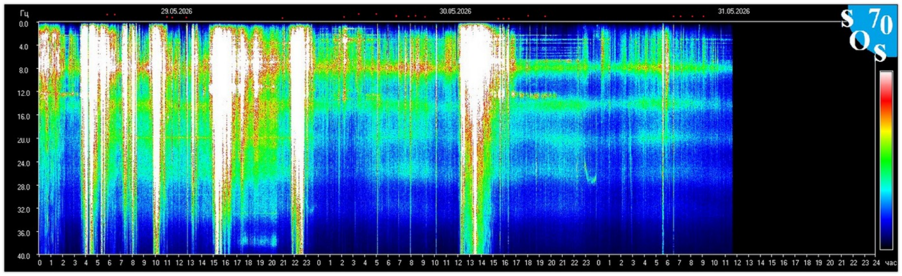

This sonogram shows Earth's natural electromagnetic resonance at approximately 7.83 Hz. Data collected from Space Observing System 70.

Plate A.9 — Tomsk S70 OS sonogram (capture date as labelled in panel header).

Sonogram Details

Captured

Jun 6, 2026, 11:51 PM CDT

Live

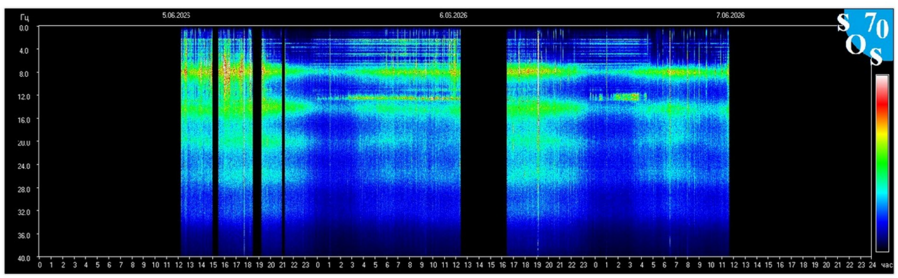

This sonogram shows Earth's natural electromagnetic resonance at approximately 7.83 Hz. Data collected from Space Observing System 70.

Plate A.10 — Tomsk S70 OS sonogram (capture date as labelled in panel header).

Captured

Jun 13, 2026, 11:50 PM CDT

Live

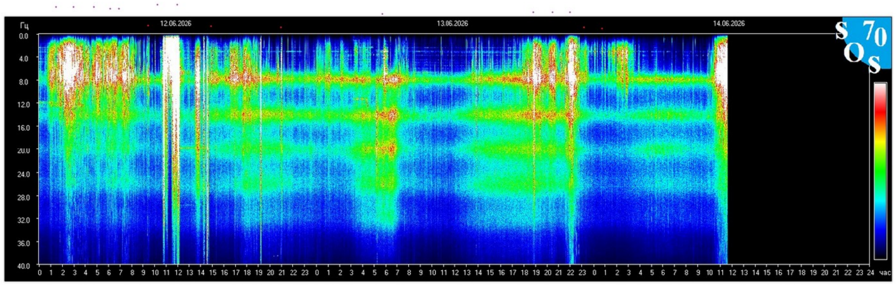

This sonogram shows Earth's natural electromagnetic resonance at approximately 7.83 Hz. Data collected from Space Observing System 70.

Plate A.11 — Tomsk S70 OS sonogram (capture date as labelled in panel header).

Sonogram Details

Captured
Jun 20, 2026, 11:50 PM CDT

Live

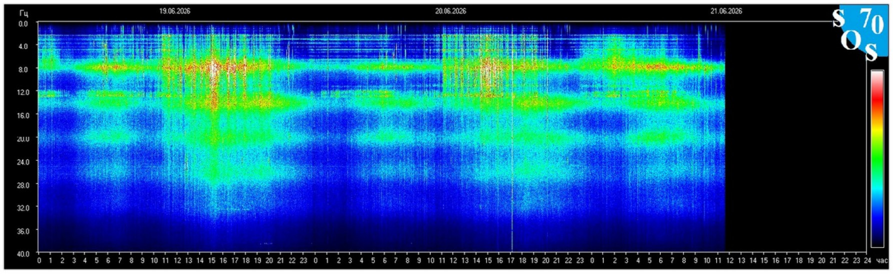

This sonogram shows Earth's natural electromagnetic resonance at approximately 7.83 Hz. Data collected from Space Observing System 70.

Plate A.12 — Tomsk S70 OS sonogram (capture date as labelled in panel header).

Captured
Jun 20, 2026, 11:50 PM CDT

Live

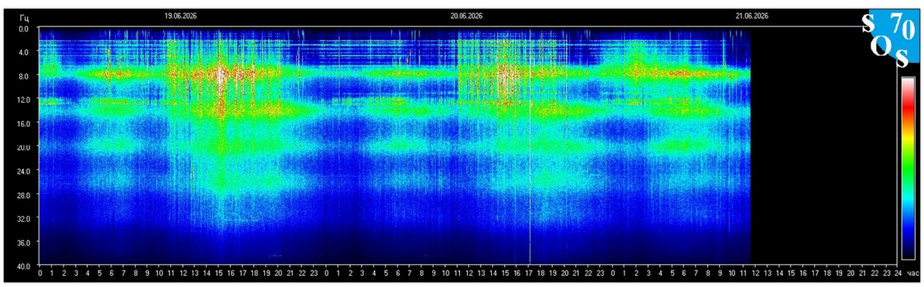

Plate A.13 — Tomsk S70 OS sonogram (capture date as labelled in panel header).

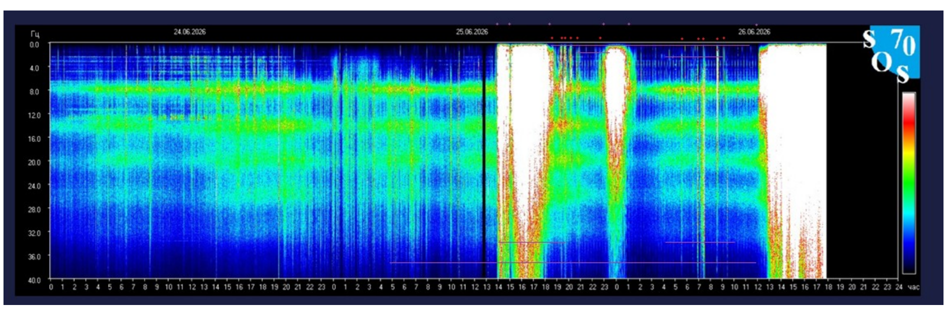

Plate A.14 — 24–26 June 2026 event window (the burst/echo sequence analysed in Experiment 1).

Appendix B — Earthquake-Catalog Provenance & Parameters

B.1 Source and queries

All earthquake data are from the USGS ANSS Comprehensive Catalog (ComCat), CSV export format, columns: time, latitude, longitude, depth, mag, magType, nst, gap, dmin, rms, net, id, updated, place, type, horizontalError, depthError, magError, magNst, status, locationSource, magSource. Times are UTC (ISO-8601). The two experiments used distinct exports:

Experiment	File(s)	Magnitude floor	Span	Rows → earthquakes
Exp 2 (pilot)	query.csv	M2.5 regional + M4.5 global	25 Mar – 26 Jun 2026	6,970 → 6,944
Exp 3 (re-test)	query_1_.csv	M4.5 global	25 Mar 2025 – 26 Mar 2026	8,557
	query_2_.csv	M4.5 global	25 Mar 2024 – 26 Mar 2025	6,565
	query_4_.csv	M4.5 global	25 Mar 2020 – 26 Mar 2021	7,545
	query_3_.csv	(empty query)	—	0
	combined, deduped	M4.5 global	2020–21 + 2024–26	22,667 → 22,635 eq
Exp 4 (triads)	query.csv + query_1_… query_9_ (10 files)	M2.5 regional + M4.5 global	2020–26 (2022–23 missing)	142,131 → 139,801 eq

B.2 Declustering results (Gardner–Knopoff 1974)

Windows: distance d = 10^(0.1238M + 0.983) km; time t = 10^(0.5409M − 0.547) d for M < 6.5, else 10^(0.032M + 2.7389) d. Largest events claim smaller events within the space–time window as dependent (haversine distances). Independent-event counts by subset:

Subset	Exp 2 (93-day) N	Exp 3 (3-year) N
All declustered	2,658	8,151
M ≥ 4.5 declustered	868	8,151
M ≥ 4.5 shallow ≤60 km	612	6,030
M ≥ 5.0 declustered	271	2,587
M ≥ 5.5 declustered	—	853
(Exp 3 island A, 2020–21 / island B, 2024–26)	—	2,955 / 5,196

B.4 Experiment 5 (octave-comb) and Experiment 6 (solar) data

Experiment 5: continuous seismic waveforms from IRIS/EarthScope — Pinyon Flat (very-broadband, VHZ 0.1 Hz; one LHZ cross-check) and Black Forest Observatory. Comb fundamental f_0 = 2.005 mHz (light-crossing time of 1 AU); octave teeth at $f_0 \cdot 2^k$; control teeth at 3, 5, 6, 7×f_0. Detector: matched filter on the whitened averaged spectrum (running-median background skipping tooth neighbourhoods), two statistics (summed octave power; count of teeth above the 95th off-comb percentile), bootstrap significance, robust de-glitching. Windows: 2006 Tonga (positive control), May 2024 (X8.7), Oct 2024 (X9.0), Apr–May 2026 (M7.5 Sanriku), 2023 Black Forest cross-check.

Experiment 6: solar-flare catalogue as tabulated in Experiment 5 §3 (eight major flares, 2020–2026); receiver Tomsk S70 OS (56.5°N, 85.0°E); day/night from astropy solar elevation (night = Sun < −6°); clean window = receiver-night and > 3 d from any major flare. Triads from the full 2020–2026 catalogue (Appendix B.1). Geomagnetic Kp/Dst (OMNIWeb) noted as the un-modelled third axis.

B.3 Constituent and ephemeris parameters

Constants: GM_moon = 4902.8, GM_sun = 1.32712440×10^{8} km^3/s^2 (degree-2 tidal potential). Lunar hour angle H_moon = GMST + east-longitude − RA_moon; H_sun analogously. Constituent phases (degrees, mod 360): M2 = 2·H_moon (lunar 12.42 h); S2 = 2·H_sun (solar 12.00 h); O1 = H_moon (lunar diurnal 25.8 h); S1 = H_sun (solar diurnal 24.0 h); synodic = λ_moon − λ_sun (spring–neap 29.53 d); fortnightly = 2×synodic (14.77 d). Schuster: $R = |\Sigma e^{i\theta}|$, $\bar{R} = R/N$, $p = \exp(-R^2/N) = \exp(-N\cdot\bar{R}^2)$. Ephemeris: astropy get_body('moon'/'sun'), builtin solar-system ephemeris; Exp 2 on a 10-min grid, Exp 3 evaluated per event time. Validation: new moons 17 Apr/16 May/15 Jun 2026; lunar declination span ±28.7°; lunar distance $357–406\times10^3$ km; solar distance $149–152\times10^6$ km.

Appendix C — Full Constituent Results (Experiment 3)

Complete per-subset, per-constituent Schuster results for the three-year catalog. p_S = Schuster, p_MC = 20,000-draw Monte-Carlo, p_χ^2 = binned chi-square; all three agree. Mean = preferred phase (degrees).

Subset	Constituent	N	$\bar{R}$	p_S	p_MC	p_χ^2	mean°
M≥4.5	M2 lunar	8151	0.0060	0.747	0.744	0.366	297
	S2 solar	8151	0.0097	0.464	0.466	0.190	355
	O1 lunar	8151	0.0117	0.325	0.323	0.111	314
	S1 solar	8151	0.0084	0.566	0.564	0.701	200
	Msf fortnight	8151	0.0153	0.149	0.150	0.226	107
	Mm synodic	8151	0.0076	0.622	0.617	0.936	318
Shallow≤60	M2 lunar	6030	0.0059	0.813	0.808	0.781	282
	S2 solar	6030	0.0086	0.638	0.645	0.443	24
M≥5.0	M2 lunar	2587	0.0183	0.419	0.422	0.641	308
	S2 solar	2587	0.0208	0.327	0.323	0.241	63
M≥5.5	M2 lunar	853	0.0434	0.201	0.205	0.063	308
	S2 solar	853	0.0176	0.767	0.767	0.134	8

C.1 Gap-spanning replication & monthly stability

Constituent	Island A 2020–21	Island B 2024–26	Δ phase
M2 lunar	N=2955, $\bar{R}$=0.010, 330°	N=5196, $\bar{R}$=0.006, 260°	70°
S2 solar	N=2955, $\bar{R}$=0.008, 316°	N=5196, $\bar{R}$=0.012, 9°	53°

Synodic-month stability (Island B, 25 contiguous months): preferred phase scatters with circular spread ~104° (random ≈ 81°, locked ≈ 0°); one anomalous month ($\bar{R}$ = 0.30, $p < 0.001$) whose phase matches none of the others. Local-solar-time-of-day: M≥4.5 χ^2 p = 0.49 (flat); M≥5.5 p = 0.23. No detection-clock structure survives at full power.

Appendix D — Analysis Code (all pipelines)

The complete Python pipeline for the definitive three-year test (Python 3, astropy 8.0, numpy/scipy/pandas). Experiment 2 used an equivalent pipeline differing only in a gridded rather than per-event ephemeris (Exp 2 §3). Run in order: p1 (decluster) → p2 (ephemeris + phases) → p3 (Schuster + diagnostics).

D.1 p1_decluster.py

```
import pandas as pd, numpy as np, time

df = pd.read_pickle('/home/claude/raw_combined.pkl')  # already earthquakes only, deduped, sorted
df = df.dropna(subset=['time','latitude','longitude','depth','mag']).reset_index(drop=True)
epoch = df['time'].min()
df['t_days'] = (df['time'] - epoch).dt.total_seconds() / 86400.0

def haversine_km(lat1, lon1, lat2, lon2):
    R = 6371.0
    p1, p2 = np.radians(lat1), np.radians(lat2)
    dphi = np.radians(lat2 - lat1); dlmb = np.radians(lon2 - lon1)
    a = np.sin(dphi/2)**2 + np.cos(p1)*np.cos(p2)*np.sin(dlmb/2)**2
    return 2*R*np.arcsin(np.sqrt(np.clip(a, 0, 1)))

def gk_windows(M):
    d = 10**(0.1238*M + 0.983)
    t = np.where(M >= 6.5, 10**(0.032*M + 2.7389), 10**(0.5409*M - 0.547))
    return d, t

lat=df['latitude'].values; lon=df['longitude'].values
mag=df['mag'].values; t=df['t_days'].values
n=len(df)
Dwin,Twin=gk_windows(mag)
order=np.argsort(-mag, kind='mergesort')
dependent=np.zeros(n, dtype=bool)
idx_all=np.arange(n)
t0=time.time()
for k,i in enumerate(order):
    if dependent[i]: continue
    dt=np.abs(t-t[i])
    cand=(mag<=mag[i])&(dt<=Twin[i])&(~dependent); cand[i]=False
    if not cand.any(): continue
    idx=idx_all[cand]
    dd=haversine_km(lat[i],lon[i],lat[idx],lon[idx])
    dependent[idx[dd<=Dwin[i]]]=True
print(f"decluster loop done in {time.time()-t0:.1f}s")

ind=~dependent
df['independent']=ind
print(f"Clean earthquakes        : {n}")
print(f"Span                     : {df['time'].min()}  ->  {df['time'].max()}")
print(f"Independent (mainshocks) : {ind.sum()}  ({100*ind.mean():.1f}%)")
print(f"Dependent (after/fore)   : {(~ind).sum()}  ({100*(~ind).mean():.1f}%)")

for label, mask in [
    ("ALL declustered",            df['independent']),
    ("M>=4.5 declustered",         df['independent'] & (df['mag']>=4.5)),
    ("M>=4.5 shallow(<=60km)",     df['independent'] & (df['mag']>=4.5) & (df['depth']<=60)),
    ("M>=5.0 declustered",         df['independent'] & (df['mag']>=5.0)),
```

```
    ("M>=5.5 declustered",         df['independent'] & (df['mag']>=5.5)),
]:
    print(f"  {label:28s}: N = {int(mask.sum())}")

# island membership for replication tests
df['island'] = np.where(df['time'] < pd.Timestamp('2023-01-01', tz='UTC'), 'A_2020_21', 'B_2024_26')
print("\nIndependent events per island:")
print(df[df['independent']].groupby('island').size())

df.to_pickle('/home/claude/catalog_clean3.pkl')
print("\nsaved catalog_clean3.pkl")
```

D.2 p2_ephem_phases.py

```
import pandas as pd, numpy as np, time
from astropy.time import Time
from astropy.coordinates import get_body, GeocentricTrueEcliptic, solar_system_ephemeris
import astropy.units as u

solar_system_ephemeris.set('builtin')

df = pd.read_pickle('/home/claude/catalog_clean3.pkl')
ind = df[df['independent']].copy().reset_index(drop=True)
print(f"Independent events to phase: {len(ind)}")

# unix seconds -> astropy Time (avoid the pandas3 int64-microsecond trap: use .timestamp())
unix = ind['time'].map(lambda x: x.timestamp()).values
t = Time(unix, format='unix', scale='utc')

t0=time.time()
# GMST in degrees
gmst_deg = t.sidereal_time('mean', 'greenwich').to(u.deg).value

# bodies in GCRS
moon = get_body('moon', t)
sun  = get_body('sun', t)
moon_ra = moon.ra.deg; moon_dec = moon.dec.deg
sun_ra  = sun.ra.deg;  sun_dec  = sun.dec.deg

# ecliptic longitudes (geocentric true ecliptic of date)
moon_ecl = moon.transform_to(GeocentricTrueEcliptic(equinox=t)).lon.deg
sun_ecl  = sun.transform_to(GeocentricTrueEcliptic(equinox=t)).lon.deg
print(f"ephemeris computed in {time.time()-t0:.1f}s")

lon_e = ind['longitude'].values  # east-positive degrees

def wrap360(x): return np.mod(x, 360.0)

# Local hour angles (degrees): H = GMST + east_longitude - RA
H_moon = wrap360(gmst_deg + lon_e - moon_ra)
H_sun  = wrap360(gmst_deg + lon_e - sun_ra)

# Tidal constituent phases (degrees)
ind['phase_M2'] = wrap360(2.0*H_moon)            # lunar semidiurnal 12.42 h  (the true body-tide line)
ind['phase_S2'] = wrap360(2.0*H_sun)             # solar semidiurnal 12.00 h  (= civil/daily clock)
ind['phase_O1'] = wrap360(H_moon)                # lunar diurnal 25.8 h
ind['phase_S1'] = wrap360(H_sun)                 # solar diurnal 24.0 h
```

```
syn = wrap360(moon_ecl - sun_ecl)                # synodic elongation (new=0, full=180)
ind['phase_syn'] = syn                           # spring-neap / monthly 29.53 d
ind['phase_Msf'] = wrap360(2.0*syn)              # synodic fortnightly 14.77 d

# local solar time (hours) for detection-artifact probe
ind['local_solar_hr'] = wrap360(H_sun + 180.0)/15.0   # 0..24, noon when sun on meridian (H=0 -> 12h)

# store helper angles
ind['H_moon']=H_moon; ind['H_sun']=H_sun
ind['moon_dec']=moon_dec; ind['sun_dec']=sun_dec
ind['syn_deg']=syn

ind.to_pickle('/home/claude/catalog_phases3.pkl')
print("saved catalog_phases3.pkl")

# sanity: new moon check (syn near 0 or 360) should align with known new moons
print("\nSanity — synodic phase distribution should be ~uniform over a multi-year span:")
hsyn,_=np.histogram(syn, bins=12, range=(0,360))
print("  12-bin counts:", hsyn, " (flat ~ uniform sampling of lunar age, expected)")
print(f"  lunar dec range: {moon_dec.min():.1f}..{moon_dec.max():.1f} deg (should be ~ +/-28.5)")
```

D.3 p3_analyze.py

```
import pandas as pd, numpy as np

rng = np.random.default_rng(42)
ind = pd.read_pickle('/home/claude/catalog_phases3.pkl')

def resultant(phase_deg):
    th = np.radians(phase_deg.values if hasattr(phase_deg,'values') else phase_deg)
    C = np.cos(th).sum(); S = np.sin(th).sum(); n=len(th)
    R = np.hypot(C,S); Rbar = R/n
    mean = np.degrees(np.arctan2(S,C)) % 360
    return Rbar, mean, n

def schuster_p(Rbar, n):          # p = exp(-R^2/n) = exp(-n*Rbar^2)
    return np.exp(-n*Rbar**2)

def mc_p(phase_deg, nmc=20000):   # uniform-null Monte Carlo on R̄
    th = np.radians(phase_deg.values if hasattr(phase_deg,'values') else phase_deg)
    n=len(th); Rbar0=np.hypot(np.cos(th).sum(),np.sin(th).sum())/n
    sims = rng.uniform(0,2*np.pi,size=(nmc,n))
    Rb = np.hypot(np.cos(sims).sum(1),np.sin(sims).sum(1))/n
    return (np.sum(Rb>=Rbar0)+1)/(nmc+1)

def chi2_p(phase_deg, nb=12):
    from scipy.stats import chisquare
    h,_=np.histogram(phase_deg, bins=nb, range=(0,360))
    return chisquare(h).pvalue

constits = [('M2','phase_M2','lunar 12.42h'),
            ('S2','phase_S2','solar 12.00h'),
            ('O1','phase_O1','lunar 25.8h'),
            ('S1','phase_S1','solar 24.0h'),
            ('Msf','phase_Msf','fortnightly 14.8d'),
            ('syn','phase_syn','synodic-month 29.5d')]
```

```
subsets = [
    ('M>=4.5 declustered',        ind),
    ('M>=4.5 shallow <=60km',     ind[ind['depth']<=60]),
    ('M>=5.0 declustered',        ind[ind['mag']>=5.0]),
    ('M>=5.5 declustered',        ind[ind['mag']>=5.5]),
]

print("="*104)
print(f"{'subset':24s} {'constit':22s} {'N':>5s} {'Rbar':>7s} {'p_Schus':>9s} {'p_MC':>8s} {'p_chi2':>8s}
{'mean°':>6s}")
print("-"*104)
rows=[]
for sname, sdf in subsets:
    for cname,col,desc in constits:
        Rbar,mean,n = resultant(sdf[col])
        ps = schuster_p(Rbar,n)
        pm = mc_p(sdf[col])
        pc = chi2_p(sdf[col])
        flag = ' *' if ps<0.01 else ''
        kind = 'LUNAR' if cname in ('M2','O1') else ('SOLAR' if cname in ('S2','S1') else 'longP')
        print(f"{sname:24s} {cname+' '+desc:22s} {n:5d} {Rbar:7.4f} {ps:9.4f} {pm:8.4f} {pc:8.4f}
{mean:6.0f}{flag}")

rows.append(dict(subset=sname,constit=cname,kind=kind,N=n,Rbar=Rbar,p=ps,pMC=pm,pchi2=pc,mean=mean))
    print()

res = pd.DataFrame(rows)
res.to_pickle('/home/claude/results3.pkl')

# ---- M2/S2 amplitude ratio (the physical discriminator) ----
print("="*104)
print("PHYSICAL DISCRIMINATOR  (real body tide => M2 ~ 2x S2 ; solar/civil clock => S2 >> M2)")
for sname,sdf in subsets:
    m2,_,n = resultant(sdf['phase_M2']); s2,_,_ = resultant(sdf['phase_S2'])
    print(f"  {sname:24s}  R̄(M2 lunar)={m2:.4f}  R̄(S2 solar)={s2:.4f}  ratio M2/S2={m2/s2:5.2f}")

# ---- gap-spanning replication: island A (2020-21) vs island B (2024-26) ----
print("="*104)
print("GAP-SPANNING REPLICATION  (3-yr gap between islands; a real constituent must agree in phase)")
A = ind[ind['island']=='A_2020_21']; B = ind[ind['island']=='B_2024_26']
for cname,col,desc in [('M2','phase_M2','lunar'),('S2','phase_S2','solar')]:
    ra,ma,na = resultant(A[col]); rb,mb,nb = resultant(B[col])
    dphi = abs((ma-mb+180)%360-180)
    print(f"  {cname} {desc:6s}:  A(2020-21) N={na} R̄={ra:.4f} ph={ma:3.0f}°   |   B(2024-26) N={nb}
R̄={rb:.4f} ph={mb:3.0f}°   |   Δphase={dphi:3.0f}°")

# ---- time-of-day (detection-artifact probe) ----
print("="*104)
print("LOCAL-SOLAR-TIME-OF-DAY  (flat => no detection clock; day/night structure => solar artifact)")
from scipy.stats import chisquare
for sname,sdf in subsets:
    h,_=np.histogram(sdf['local_solar_hr'],bins=24,range=(0,24))
    pc=chisquare(h).pvalue
    peak=h.argmax(); trough=h.argmin()
    print(f"  {sname:24s} N={len(sdf):5d}  χ²p={pc:7.4f}  peak~{peak:02d}h({h[peak]})
trough~{trough:02d}h({h[trough]})  max/min={h[peak]/max(h[trough],1):.2f}")
```

```
# ---- monthly per-cycle replication over the full set of synodic months ----
print("="*104)
print("SYNODIC-MONTH PHASE STABILITY  (does the 'monthly' preferred phase repeat across many cycles?)")
sdf = ind  # M>=4.5
# assign each event to a synodic month index using continuous lunar age accumulated: use time since epoch
/ 29.53
unix = sdf['time'].map(lambda x:x.timestamp()).values
t_days = (unix-unix.min())/86400.0
# only meaningful within continuous coverage; report island B (2 contiguous yrs) cycle-by-cycle
B = sdf[sdf['island']=='B_2024_26'].copy()
ub = B['time'].map(lambda x:x.timestamp()).values
tb=(ub-ub.min())/86400.0
cyc = (tb//29.53).astype(int)
B['cyc']=cyc
phases=[]
for c in range(cyc.max()+1):
    sub=B[B['cyc']==c]
    if len(sub)<30: continue
    r,m,n=resultant(sub['phase_syn'])
    phases.append(m)
    if c<6 or c%6==0:
        print(f"  B cycle {c:2d}: N={n:4d} R̄={r:.3f} preferred_phase={m:3.0f}°  p={schuster_p(r,n):.3f}")
phases=np.array(phases)
# circular std of per-cycle preferred phases: small => stable/real, ~104° => random
cm=np.degrees(np.arctan2(np.sin(np.radians(phases)).mean(),np.cos(np.radians(phases)).mean()))%360
Rc=np.hypot(np.cos(np.radians(phases)).mean(),np.sin(np.radians(phases)).mean())
circ_std=np.degrees(np.sqrt(-2*np.log(Rc))) if Rc>0 else np.inf
print(f"  -> across {len(phases)} contiguous months: mean preferred phase={cm:.0f}°, circular
spread={circ_std:.0f}° (random≈81°, locked≈0°)")
```

D.4 triad_census.py (Experiment 4)

```
import pandas as pd, numpy as np

eq = pd.read_pickle('/home/claude/full_catalog.pkl')
eq = eq.dropna(subset=['mag','time']).sort_values('time').reset_index(drop=True)
t = eq['time'].map(lambda x:x.timestamp()).values  # unix seconds

def triad_clusters(mask, window_h):
    """Non-overlapping count of windows containing >=3 events of the masked set."""
    idx = np.where(mask)[0]
    if len(idx)<3: return 0, []
    tt = t[idx]
    W = window_h*3600
    clusters=[]; i=0; n=len(tt)
    while i <= n-3:
        # does a triad start at i? (3rd event within window of 1st)
        if tt[i+2]-tt[i] <= W:
            # extend cluster: include all subsequent events within W of the cluster start
            j=i+2
            while j+1<n and tt[j+1]-tt[i] <= W:
                j+=1
            clusters.append((idx[i], idx[j], int(j-i+1)))
            i=j+1  # advance past this cluster (non-overlapping)
        else:
            i+=1
    return len(clusters), clusters
```

```
cover_years = 5.0  # ~5 yr actual coverage (2020-22 + 2023-26, one yr gap)
print(f"Catalog: {len(eq)} eq, 2020-2026 (~{cover_years:.0f} yr coverage, 2022-23 missing)\n")
print("TRIAD CENSUS  \u2014 number of distinct windows containing \u22653 quakes \u2265 threshold")
print(f"{'min mag':>8} | {'2 h':>18} | {'8 h':>18} | {'24 h':>18}")
print("-"*72)
rows=[]
for thr in [5.5,6.0,6.5,7.0]:
    mask = eq['mag'].values >= thr
    nE = int(mask.sum())
    cells=[]
    for W in [2,8,24]:
        c,_ = triad_clusters(mask, W)
        cells.append(c)
        rows.append((thr,W,c,nE))
    print(f"{thr:>8.1f} | {cells[0]:>4d} ({cells[0]/cover_years:>4.1f}/yr) | {cells[1]:>4d}
({cells[1]/cover_years:>4.1f}/yr) | {cells[2]:>4d} ({cells[2]/cover_years:>4.1f}/yr)   [N\
u2265thr={nE}]")

print("\nKey reference \u2014 the June-24-2026 triad magnitudes were M5.6, M6.9, M7.5 (span ~1.5 h).")
print("  At M\u22655.5 it is a triad; at M\u22656.5 only two events qualify (a doublet).\n")

# Characterize the notable large triads (M>=6.5, 8h) by listing them
mask = eq['mag'].values >= 6.5
_, cl = triad_clusters(mask, 8)
print(f"All M\u22656.5 triads within 8 h, 2020-2026 ({len(cl)} found):")
for a,b,k in cl:
    sub = eq.iloc[a:b+1]
    sub = sub[sub['mag']>=6.5]
    span_h = (t[b]-t[a])/3600
    mags = ",".join(f"{m:.1f}" for m in sub['mag'].values)
    places = "; ".join(sub['place'].astype(str).str[:22].values[:4])
    print(f"  {sub['time'].iloc[0].date()}  span {span_h:4.1f}h  k={k}  M[{mags}]")

# How often is ANY given day a "triad day" at M>=5.5/8h (base rate)?
mask55 = eq['mag'].values>=5.5
c55,_ = triad_clusters(mask55,8)
days_total = (t[-1]-t[0])/86400 - 363  # subtract the gap
print(f"\nBase rate at M\u22655.5/8h: {c55} triads over ~{days_total:.0f} covered days "
      f"= one roughly every {days_total/max(c55,1):.0f} days.")
```

D.5 solar_interference.py (Experiment 6)

```
import pandas as pd, numpy as np
from astropy.time import Time
from astropy.coordinates import EarthLocation, AltAz, get_sun
import astropy.units as u

eq =
pd.read_pickle('/home/claude/full_catalog.pkl').dropna(subset=['mag','time']).sort_values('time').reset_i
ndex(drop=True)
t = eq['time'].map(lambda x:x.timestamp()).values

# --- flare catalog (user-provided table + the Oct-2024 X9.0 from the octave-comb report) ---
flares = pd.DataFrame([
    ("2020-11-29","M4.4",4.4,"largest eruption of 2020 (cycle infancy)"),
    ("2021-07-03","X1.5",15,"first X-class flare of Solar Cycle 25"),
```

```
    ("2022-04-20","X2.2",22,"transition into hyperactive phase"),
    ("2023-12-31","X5.0",50,"New Year's Eve eruption"),
    ("2024-05-14","X8.7",87,"strongest flare of solar maximum (AR3664, Gannon)"),
    ("2024-10-03","X9.0",90,"strongest flare of the cycle (Oct 2024, +severe storm)"),
    ("2025-11-15","X5.16",51.6,"massive CME ~1,950 km/s (date approx: month only given)"),
    ("2026-02-01","X8.3",83,"AR4366; HF radio blackouts Australia/NZ"),
], columns=['date','cls','score','note'])
flares['t']=pd.to_datetime(flares['date'],utc=True).map(lambda x:x.timestamp())
print("Flare catalog (X-ray class score = 10*X-number, M=class number):")
for _,r in flares.iterrows(): print(f"  {r['date']}  {r['cls']:6s}  {r['note']}")

# --- Schumann receiver: Tomsk S70 OS (source of the spectrograms) ---
TOMSK = EarthLocation(lat=56.5*u.deg, lon=85.0*u.deg, height=130*u.m)
def sun_elev(unix_times):
    tt=Time(np.atleast_1d(unix_times),format='unix')
    altaz=get_sun(tt).transform_to(AltAz(obstime=tt,location=TOMSK))
    return altaz.alt.deg

# --- triad finder (reuse) ---
def triad_clusters(mask, window_h):
    idx=np.where(mask)[0]
    if len(idx)<3: return []
    tt=t[idx]; W=window_h*3600; out=[]; i=0; n=len(tt)
    while i<=n-3:
        if tt[i+2]-tt[i]<=W:
            j=i+2
            while j+1<n and tt[j+1]-tt[i]<=W: j+=1
            out.append((idx[i],idx[j])); i=j+1
        else: i+=1
    return out

NIGHT_ELEV=-6.0   # sun below civil twilight = "night" at receiver
FLARE_WIN=3.0     # days; a major flare within this window = contaminated

def classify(thr, W):
    cl=triad_clusters(eq['mag'].values>=thr, W)
    rows=[]
    for a,b in cl:
        sub=eq.iloc[a:b+1]; big=sub.loc[sub['mag'].idxmax()]
        tref=t[sub['mag'].values.argmax()+a]
        elev=float(sun_elev(tref)[0])
        dflare=float(np.min(np.abs(flares['t'].values - tref))/86400.0)
        night = elev < NIGHT_ELEV
        flare_clean = dflare > FLARE_WIN
        rows.append(dict(date=str(big['time'].date()), maxmag=float(big['mag']),
                         elev=elev, night=night, dflare=dflare, flare_clean=flare_clean,
                         clean=(night and flare_clean), place=str(big['place'])[:30]))
    return pd.DataFrame(rows)

print("\n=== CLEAN-WINDOW CLASSIFICATION (receiver=Tomsk; night=sun<-6°; flare-clean=>3 d from major
flare) ===")
for thr,W in [(6.0,8),(6.5,8)]:
    df=classify(thr,W)
    nC=int(df['clean'].sum()); nN=int(df['night'].sum()); nF=int(df['flare_clean'].sum())
    print(f"\nM\u2265{thr}/{W}h triads: {len(df)} total | night {nN} | flare-clean {nF} | BOTH (clean)
{nC} ({100*nC/max(len(df),1):.0f}%)")
    if thr==6.5:
```

```
        print("  Detailed (the rare large triads):")
        for _,r in df.iterrows():
            print(f"    {r['date']}  M{r['maxmag']:.1f}  elev={r['elev']:+5.1f}\u00b0 {'NIGHT' if
r['night'] else 'day  '}  "
                  f"flare {r['dflare']:5.1f}d {'(clean)' if r['flare_clean'] else '(near)'}  => {'CLEAN'
if r['clean'] else 'contaminated'}  [{r['place']}]")

# --- June 24 2026 reference case (postdates catalog) ---
j_echo = pd.Timestamp("2026-06-25 19:30",tz='UTC').timestamp()  # mid echo window
j_quake= pd.Timestamp("2026-06-24 22:30",tz='UTC').timestamp()
je=float(sun_elev(j_echo)[0]); jq=float(sun_elev(j_quake)[0])
jdflare=float(np.min(np.abs(flares['t'].values - j_quake))/86400.0)
print(f"\nJune 24 2026 (Exp 1 case): quake-time elev {jq:+.1f}\u00b0, echo-window elev {je:+.1f}\u00b0
({'night' if je<NIGHT_ELEV else 'day'}); "
      f"nearest flare {jdflare:.0f} d.")
print("  -> echo recorded at receiver-night and no flare within 3 d, BUT Exp 1 noted an active G1
geomagnetic storm")
print("     (Kp~5.0) - a separate contaminant. So 'flare-clean' but NOT geomagnetically clean.")

# save classification for plotting
classify(6.0,8).to_pickle('/home/claude/triads_cls60.pkl')
classify(6.5,8).to_pickle('/home/claude/triads_cls65.pkl')
flares.to_pickle('/home/claude/flares.pkl')
print("\nsaved classifications + flares")
```